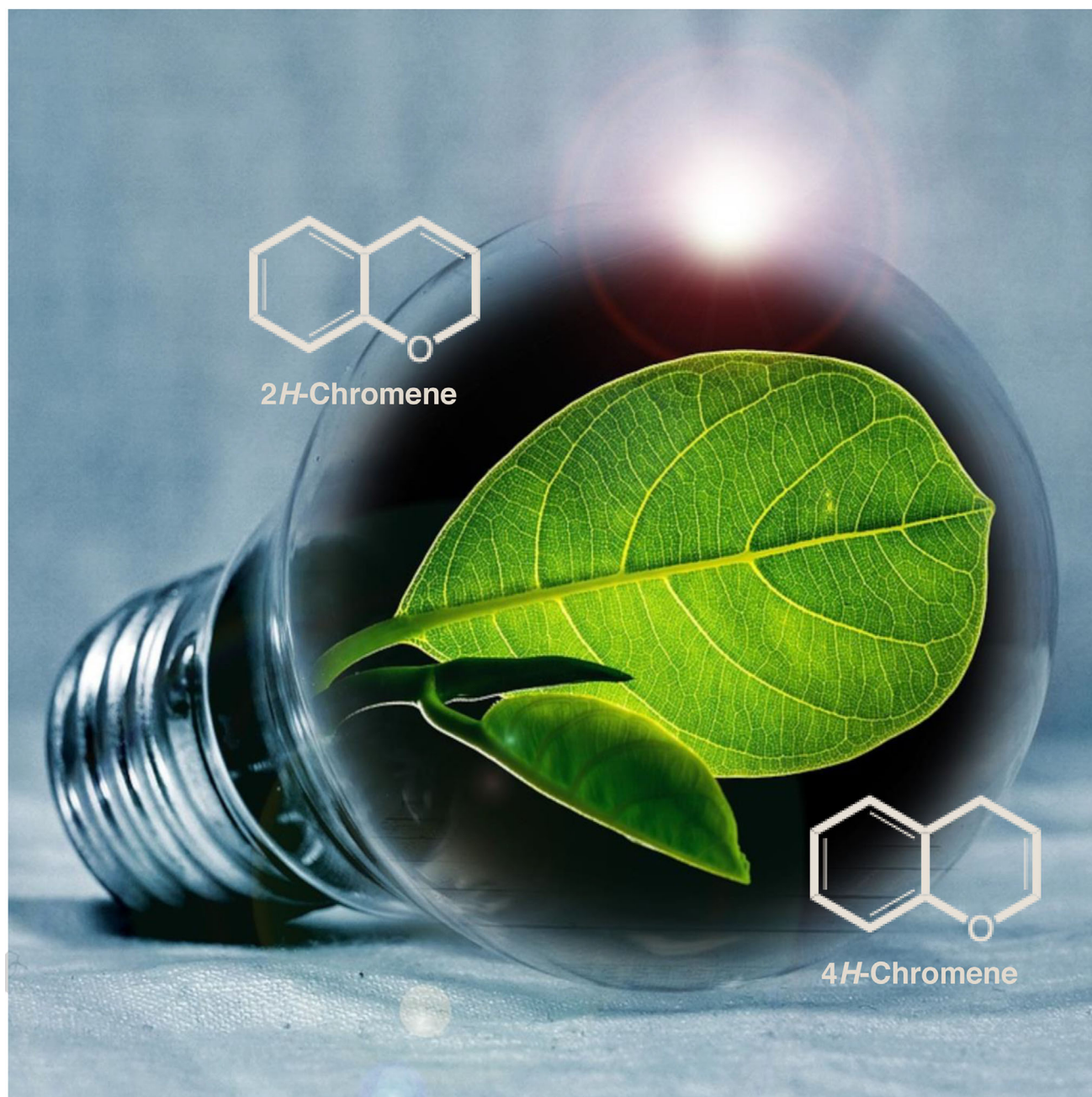


# Visible-Light Photocatalysis for Sustainable Chromene Synthesis and Functionalization

Paula Pérez-Ramos,<sup>[a]</sup> Georgia Biniari,<sup>[b]</sup> Raquel G. Soengas,<sup>[a]</sup> Humberto Rodríguez-Solla,<sup>[a]</sup> and Carmen Simal<sup>\*[b]</sup>



Chromenes represent a biologically significant family of heterocycles, widely present in pharmaceutical compounds and secondary metabolites. Their importance in synthesis and medicinal chemistry has driven continuous efforts to develop advanced and efficient synthetic methodologies. Over the past decade, photoredox catalysis has revolutionized Organic Synthesis, offering innovative and sustainable strategies for the construction and functionalization of complex molecules. The synthesis of

chromene derivatives has greatly benefited from the integration of visible-light-promoted methodologies, which utilize light as an abundant and non-toxic energy source, enabling greener chemical transformations. In this review, the latest progress in visible-light-mediated approaches for the synthesis of chromene derivatives, along with the photochemical reactivity of these relevant frameworks, are summarized.

## 1. Introduction

Chromenes are a prominent class of heterocyclic compounds with simple structures and a wide range of biological profiles, often serving as pharmacophores in numerous essential drugs.<sup>[1]</sup> They exhibit a broad spectrum of pharmaceutical and biological activities, including anti-inflammatory, antioxidant, antifungal, anti-Human Immunodeficiency Virus, anti-Alzheimer, and anti-cancer properties.<sup>[2]</sup> Beyond their pharmacological significance, the chromene scaffold also forms the backbone of various fluorescent molecules, particularly valuable in biological systems and material science.<sup>[3]</sup>

Chromenes are bicyclic oxygen-containing heterocycles comprising a 1-benzopyran moiety formed by a pyran ring fused to a benzene ring at the 5,6-position. These structures give rise to four common structural motifs, each with unique properties and potential applications, distinguished by the location of the unsaturation in the pyran ring and the presence and relative position of a carbonyl group (Figure 1). In 2*H*-chromenes, the double bond is at the 3,4-position within the pyran ring, whereas 4*H*-chromenes display the double bond at the 2,3-position. 4*H*-chromen-4-ones and 2*H*-chromen-2-ones, which are characterized by having a carbonyl function, are usually denoted as chromones and coumarins, respectively.

Given their importance, there has been a continuous focus on developing general, straightforward, and efficient synthetic strategies to prepare chromene derivatives.<sup>[4]</sup> However, the growing emphasis on more sustainable chemical processes

has revealed the limitations of traditional methods in aligning with green chemistry for chromene synthesis. Therefore, the challenge of achieving more convenient and environmentally friendly approaches to achieve chromene analogs from readily available starting materials has become a significant area of interest.

Photocatalysis has emerged as a powerful synthetic tool in organic chemistry, offering new ways to access reactive intermediates under mild conditions.<sup>[5]</sup> Through photoredox catalysis, visible light is efficiently converted into chemical energy using photoexcitable catalysts, which allows the catalytic generation of reactive radical species without the need for harsh reagents or extreme conditions.<sup>[6]</sup> A key factor in the rapid progression of this field has been the discovery of metal complexes and organic photocatalysts capable of harnessing visible light to facilitate single-electron transfer (SET) processes under exceptionally mild conditions. Nowadays, synthetic chemists have at their disposal a wide variety of organometallic and organic photocatalysts with different photophysical and electrochemical properties, which allow their reactivity to be tuned (Figure 2).

Upon excitation, these catalysts can participate in SET events with organic/organometallic substrates, enabling the formation of highly reactive species and unlocking bond disconnections previously unattainable through traditional two-electron pathways. Here, irradiation with visible light, at wavelengths where common organic molecules do not absorb, results in a selective excitation of the photoredox catalyst. The resulting excited species can simultaneously act as strong oxidants and strong reducers, which is unique in Organic Chemistry. In fact, this electronic duality is in direct contrast to traditional redox reactions where the reaction medium can be either oxidizing or reducing (but not both), thereby giving access to previously inaccessible neutral redox reactions (Scheme 1). Moreover, the radical species generated upon visible-light irradiation can trigger cascade processes, delivering complex and densely functionalized cyclic architectures in a single step and with high efficiency.<sup>[7]</sup>

Along with its synthetic advantages, photocatalysis brings clear benefits for sustainability, fulfilling several principles of Green Chemistry and promoting greener opportunities for organic synthesis.<sup>[8]</sup> By using light as an energy source, chemical transformations are conducted more efficiently, minimizing the use of harmful reagents and reducing waste generation.

With the increasing interest in photocatalysis for its ability to facilitate more eco-friendly chemical processes, researchers have

[a] P. Pérez-Ramos, R. G. Soengas, H. Rodríguez-Solla  
Department of Organic and Inorganic Chemistry, and Instituto Universitario de Química Organometálica Enrique Moles, University of Oviedo, Julián Clavería 8, Oviedo33006, Spain

[b] G. Biniari, C. Simal  
Department of Chemistry (Division of Organic Chemistry, Biochemistry, and Natural Products), University of Patras, University Campus, Patras26504, Greece  
E-mail: csimal@upatras.gr

[Correction Statement: This paper has been corrected to include the Frontispiece on April 14, 2025.]

© 2025 The Author(s). Chemistry – A European Journal published by Wiley-VCH GmbH. This is an open access article under the terms of the Creative Commons Attribution-NonCommercial-NoDerivs License, which permits use and distribution in any medium, provided the original work is properly cited, the use is non-commercial and no modifications or adaptations are made.

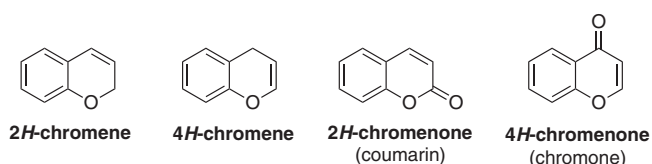


Figure 1. General structure and classification of chromenes.

turned their attention to visible-light-induced processes for the synthesis and derivatization of chromenes. This review aims to compile the contributions to this relatively new research field, providing an up-to-date, informative summary of recent visible-light-driven methods for chromene synthesis. It highlights both the development of new methodologies and the applications of chromene-derived synthons in photocatalytic transformations, offering a promising future for sustainable chromene chemistry.



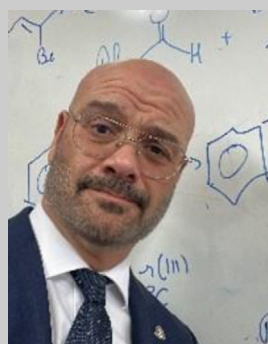
Paula Pérez-Ramos was born in Oviedo (Spain) in 1998. She earned her Master's Degree in Chemistry from the University of Oviedo in 2020. She is now pursuing her Ph.D. at the Department of Organic and Inorganic Chemistry (University of Oviedo, Spain) under the supervision of Prof. Raquel G. Soengas and Prof. Humberto Rodríguez-Solla. Her main area of study focuses on the development of new photocatalytic methodologies to achieve the synthesis of bioactive derivatives, with a special interest in flavonoids.



Georgia Biniari was born in 1996 in Greece. She received her degree in Chemistry in 2018 and her Master's Degree in Medicinal Chemistry and Chemical Biology in 2020 from the University of Patras. She completed her Ph.D. at the same university in 2024 under the supervision of Prof. Theodore Tselios. Her research encompasses organic and peptide synthesis, with focus on developing targeted therapies for hormone-dependent cancers. She has recently begun exploring flavonoid derivatives and their potential pharmaceutical interest.



Raquel Soengas was born in Lugo, (Spain) in 1975. She studied Chemistry at the University of Santiago de Compostela, where she received her Ph.D. in 2003. She joined the group of Prof. Fleet at the University of Oxford (UK) as postdoctoral researcher. In 2005, she was appointed as Assistant Professor at the University of A Coruña (Spain), where she started her independent research career. In 2021, she was appointed as Associate Professor at the University of Oviedo (Spain). She has published over 100 papers. Her research interests focus on the synthesis of pharmacologically relevant compounds using organometal-



lic reagents and photocatalyzed transformations.

Humberto Rodríguez-Solla was born in Gijón (Spain) in 1975 and graduated in Chemistry in 1998 at the University of Oviedo. He obtained his Ph.D. in Organic Chemistry at the same university in 2002. That same year, he joined the research group of Prof. Stephen G. Davies at the University of Oxford (UK) until 2005 when he was hired as Ramón y Cajal Researcher at the University of Oviedo. In 2010, he was appointed as Associate Professor and in 2021 he obtained the position of Full Professor. He has published more than 100 contributions and his current research interests are focused on the development of new synthetic methodologies using photocatalysis and organometallic reagents directed toward the synthesis of potential bioactive compounds.



Carmen Simal earned her Ph.D. in 2009 from the University of Oviedo (Spain) under Prof. J. M. Concellón and Prof. H. Rodríguez-Solla. She subsequently pursued postdoctoral research at the University of Oxford with Prof. A. Russell and at the University of St. Andrews with Prof. A. D. Smith, among others, focusing on medicinal chemistry and organocatalysis, respectively. Her research spans asymmetric synthesis, design and synthesis of bioactive compounds (small molecules/peptide-drug conjugates), and materials chemistry. Appointed as Assistant Professor at the University of Patras (Greece, 2023), she has embarked on exploring chromenone-type structures for pharmaceutical applications, emphasizing targeted drug delivery systems and innovative synthetic methodologies.



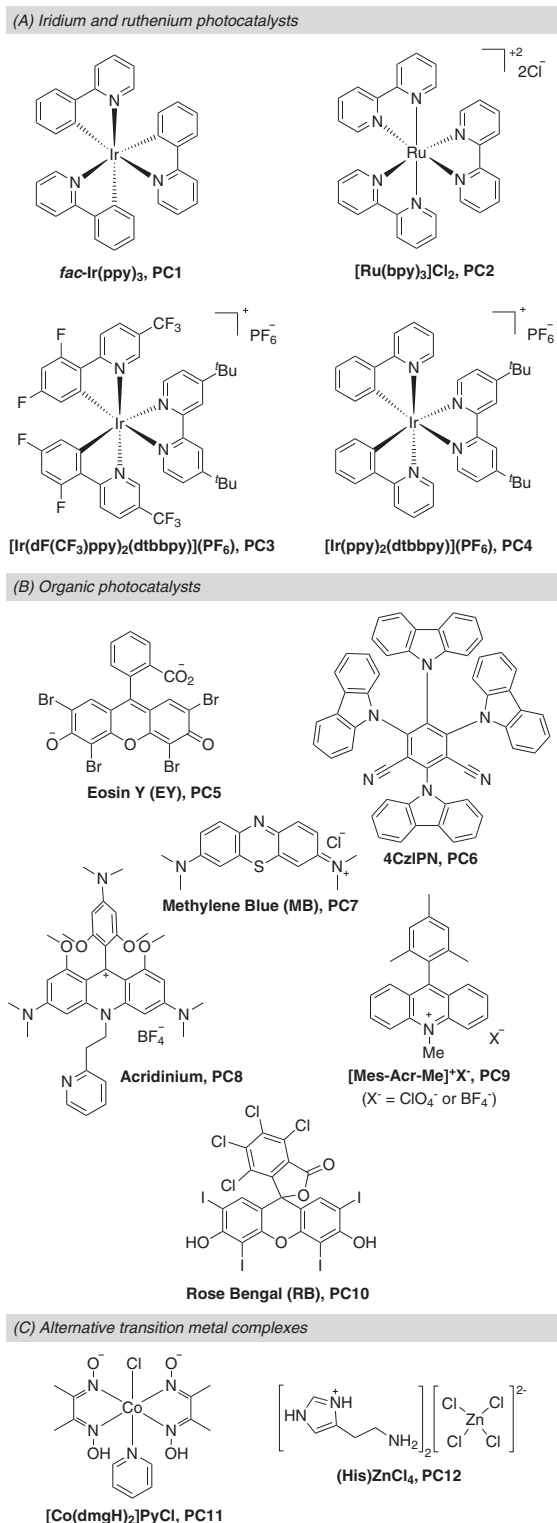
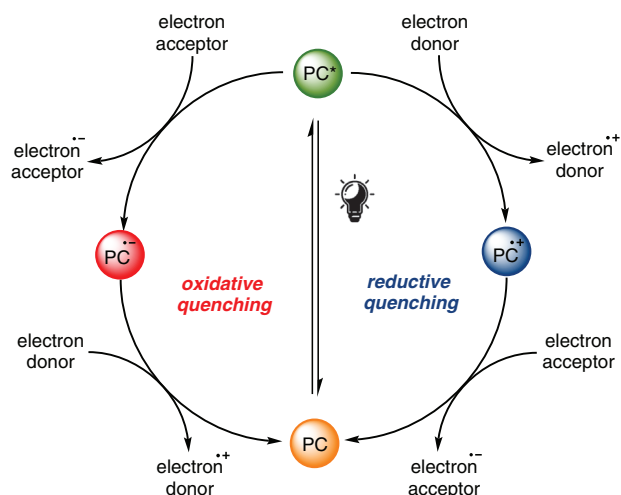


Figure 2. Structures of several relevant photocatalysts.

## 2. Visible-Light in the Synthesis of Chromene Derivatives

Considering the relevant properties of chromene derivatives, extensive efforts have been focused on developing methodologies for their synthesis.<sup>[4]</sup> Although most of these protocols



Scheme 1. General mechanism of photoredox catalysis.

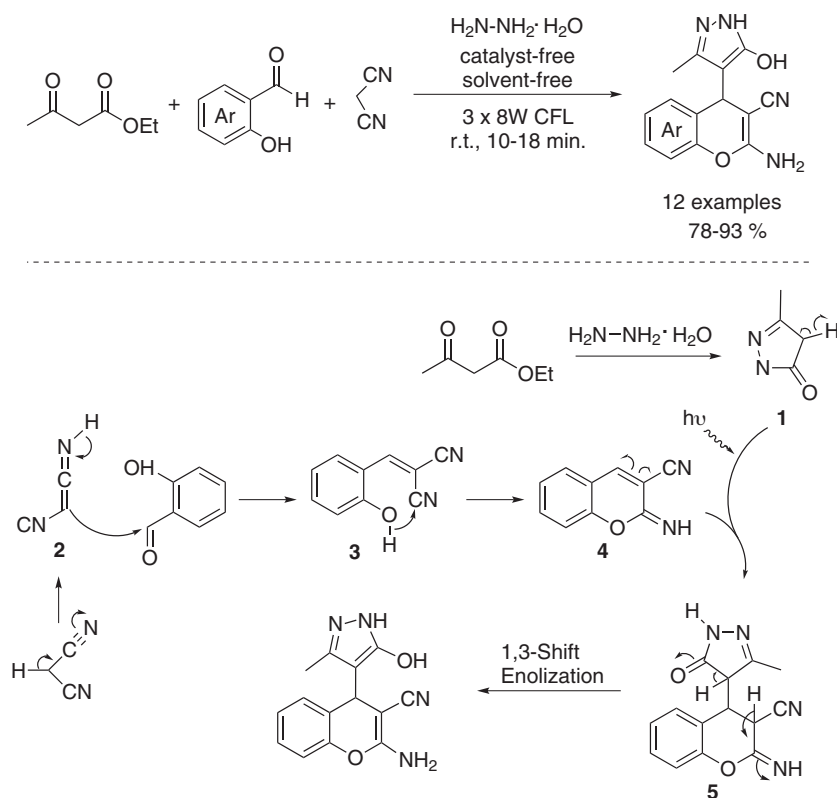
are effective, some drawbacks include long reaction times, tedious workup, high energy consumption, non-reusable mediators, and toxic reagents and solvents. Accordingly, developing greener approaches to synthesizing chromene derivatives remains a priority in addressing both environmental and economic concerns.<sup>[9]</sup>

In this context, visible light is an inexpensive, abundant, renewable, and available energy source and a non-polluting reagent with immense potential for chemical transformations. Consequently, photochemical reactions have become an appealing alternative for the sustainable preparation of chromene derivatives.

### 2.1. Synthesis of Chromenes

Among the photocatalyzed strategies developed for the construction of the chromene scaffold, visible-light-induced multicomponent reactions stand out as some of the most successful and widely applied approaches. Multicomponent reactions (MCRs) involve the formation of several bonds in a single step, offering many advantages over conventional multistep syntheses, such as improved atom economy, cost-effectiveness, energy efficiency, and minimal use of raw materials.<sup>[10]</sup> Combining these benefits with the unique features of photocatalysis results in an incredibly valuable tool for organic synthesis.<sup>[11]</sup>

In this regard, Singh and co-workers introduced the preparation of pyrazolyl-chromenes through a photoinduced multicomponent reaction.<sup>[12]</sup> By reacting salicylaldehyde derivatives, malononitrile, ethylacetoacetate, and hydrazine hydrate under 3 × 8 W compact fluorescent lamp (CFL) and solvent-free conditions, they achieved 2-amino-4-(1*H*-pyrazol-4-yl)-4*H*-chromenes in good yields (12 examples, 78–93%, Scheme 2). The proposed mechanism for this transformation is depicted below. Initially, a nucleophilic addition reaction between hydrazine and ethyl 3-oxobutanoate followed by elimination affords intermediate 1. Meanwhile, the malononitrile undergoes tautomerization in the



**Scheme 2.** Photoinduced multicomponent reaction for the preparation of pyrazoyl-chromenes and proposed mechanism.

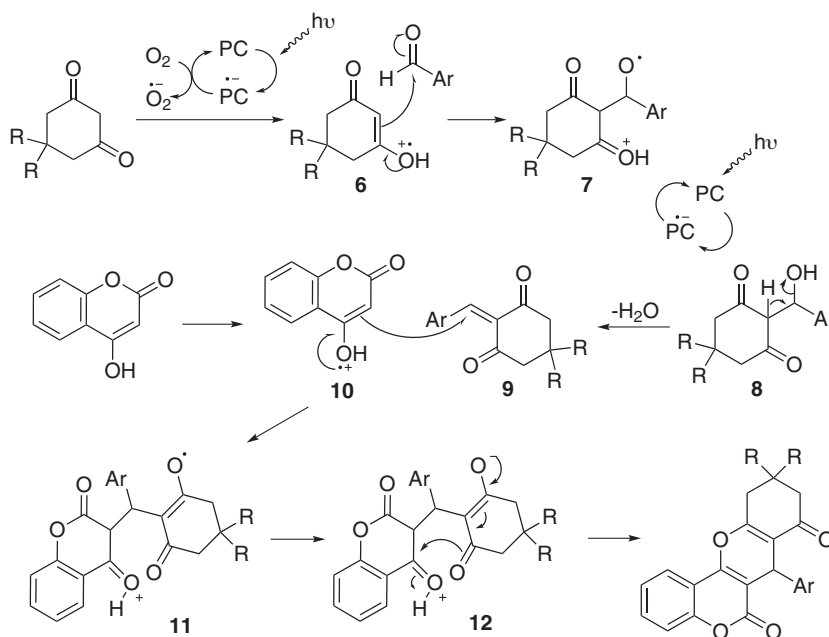
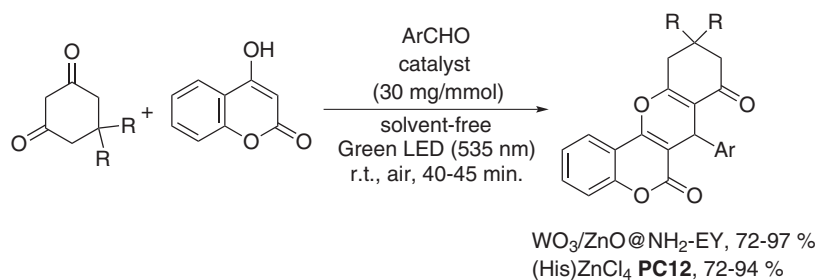
presence of visible light to give **2**, which upon Knoevenagel condensation with salicylaldehyde forms the corresponding hydroxyl benzylidenemalononitrile **3**. Subsequent intramolecular cyclization of **3** gives 2-imino-2*H*-chromene-3-carbonitrile **4**. Intermediates **1** and **4** then undergo homolytic fission in the presence of visible light, leading to their radical combination and the formation of intermediate **5**. Finally, **5** undergoes a 1,3-shift followed by enolization to afford the desired 2-amino-4-(1*H*-pyrazol-4-yl)-4*H*-chromenes (Scheme 2). The reaction runs in the absence of base, solvent, hazardous chemicals, or harsh reaction conditions and at room temperature (r.t.), making this protocol highly attractive from a sustainability perspective. Therefore, visible-light-induced MCRs have recently gained prominence as a practical tool to elaborate libraries of chromene analogs.

Singh and co-workers also reported the visible-light-induced multicomponent reaction of aryl aldehydes, 1,3-cyclohexanedione, and 4-hydroxycoumarins for the synthesis of chromeno[4,3-*b*]chromenes.<sup>[13]</sup> Building on this work, Tayebbe and his team reported a similar protocol to provide chromeno[4,3-*b*]chromenes in good yields (7 examples, 72–97%) by using an Eosin Y-supported nanocomposite (WO<sub>3</sub>/ZnO) as green heterogeneous nanocatalyst, under solventless conditions (Scheme 3).<sup>[14]</sup> The WO<sub>3</sub>/ZnO@NH<sub>2</sub>-EY nanocomposite not only exhibits high catalytic activity but also facilitates the workup and can be recovered over four times without losing catalytic activity. In a follow-up study, the same authors presented a novel histaminium tetrachlorozincate nanophotocatalyst **PC12** for the same one-pot condensation.<sup>[15]</sup> As in the previous work, the reaction proceeds under solvent-free conditions, afford-

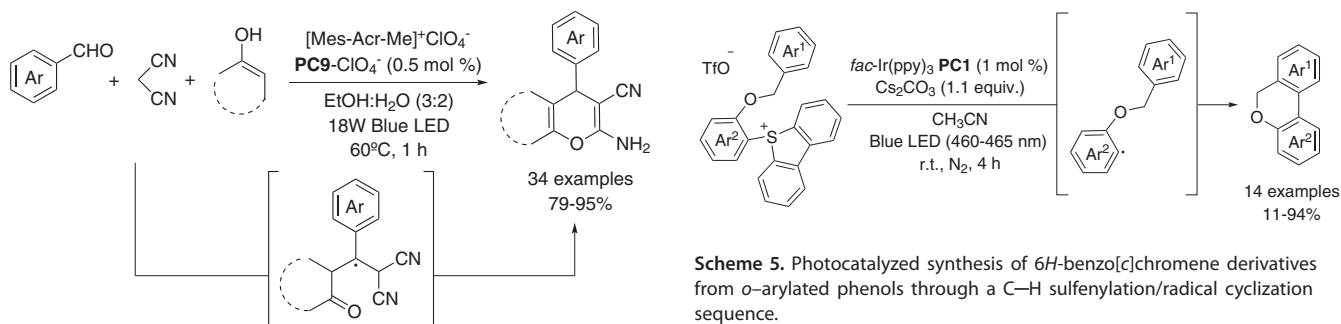
ing the desired chromeno[4,3-*b*]chromenes in good yields (6 examples, 72–94%, Scheme 3).

The proposed mechanism for this transformation involves the absorption of visible light, which excites the photoredox catalyst, leading to the generation of a superoxide species. This reactive intermediate subsequently promotes the conversion of the 1,3-dicarbonyl compound into radical cation **6**. This radical cation can react with the aromatic aldehyde to form an intermediate **7**, which is transformed into **8** via an electron transfer process promoted by the photocatalyst. The dehydration of compound **8** produces the dicarbonyl-enone **9**. Simultaneously, 4-hydroxycoumarin is converted into the radical-cation **10** via photochemical electron transfer and initiates a Michael-type addition reaction with dicarbonyl-enone **9** to provide intermediate **11**. Photochemical electron transfer reactions by the mediation of the nanophotocatalyst achieves the conversion of **11** into **12**, which finally undergoes an intramolecular condensation reaction to afford the target chromene product (Scheme 3).

Chen et al. reported another example of a photocatalyzed MCR in 2020,<sup>[16]</sup> further demonstrating its potential as a sustainable approach for the synthesis of chromenes. Thus, the one-pot formation of 2-amino-4*H*-chromenes was achieved in high yields (34 examples, 79–95%) by reacting a wide range of aromatic aldehydes with malononitrile and ArOH-type substrates, using low loadings of a 9-mesityl-10-methylacridinium photocatalyst [Mes-Acr-Me]<sup>+</sup>ClO<sub>4</sub><sup>−</sup> (**PC9**-ClO<sub>4</sub><sup>−</sup>) under blue LED irradiation (Scheme 4). Even though, unlike the previous photoinduced MCR reactions described by Singh and Tayebbe, this



**Scheme 3.** Photocatalyzed multicomponent reaction for the formation of chromeno[4,3-*b*]chromenes and proposed mechanism.



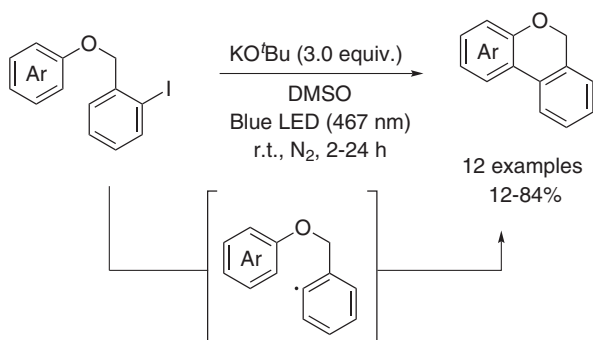
**Scheme 4.** Photocatalyzed multicomponent reaction for the synthesis of 2-amino-4*H*-chromenes.

methodology requires the presence of a solvent, it employs a green and sustainable option. Therefore, the methodology is environmentally benign and cost-effective, having the potential for broad industrial application.

Intramolecular radical cyclization offers another valuable approach for constructing the chromene ring. The use of this strategy in visible-light-mediated chromene synthesis was first reported in 2021 by Karreman et al.<sup>[17]</sup> They employed *S*-aryl dibenzothiophenium salts, obtained through a highly regioselective C–H sulfenylation of *o*-aryl-protected phenols, as pre-

cursors of 6*H*-benzo[*c*]chromene analogs (Scheme 5). The reaction starts with a photocatalytically single-electron transfer to the sulfonium salt triggered by *fac*-Ir(ppy)<sub>3</sub> (**PC1**), which promotes the formation of an aryl radical using the selective cleavage of the S–Ar<sub>exo</sub> bond. Once formed, the photo-redox-promoted radical generation initiates a Pschorr-type cyclization, leading to the desired 6*H*-benzo[*c*]chromenes (14 examples, 11–94%).

Inspired by this work, Heredia et al. described the visible-light-induced synthesis of the 6*H*-benzo[*c*]chromene ring under metal-free conditions.<sup>[18]</sup> Thus, the reaction of (2-iodobenzyl)phenyl ethers with KOT<sub>Bu</sub> under blue LED irradiation afforded the desired 6*H*-benzo[*c*]chromene derivatives with

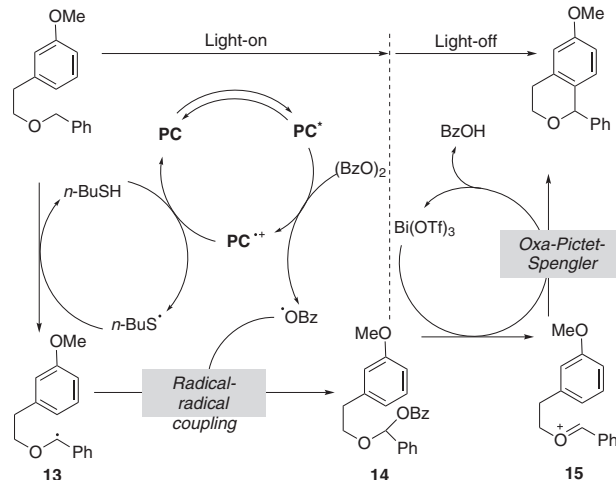
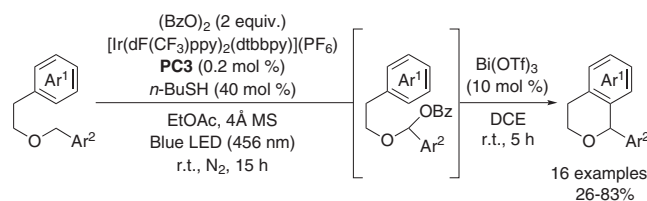


**Scheme 6.** Photocatalyzed synthesis of 6H-benzo[c]chromene derivatives from (2-halobenzyl)phenyl ethers.

good functional group tolerance (12 examples, Scheme 6). Yields were affected by the electronic properties of the substituents on the aromatic ring, with substrates containing electron-donating groups (EDGs) giving better yields (40–84%) compared to those with electron-withdrawing groups (EWGs) (12–54%). This difference in reactivity was attributed to the balance between the electron affinity (EA) of the substrate and the corresponding product. Thus, compounds with EDG exhibited lower  $\Delta$ EA, resulting in higher yields, whereas those with EWG showed higher  $\Delta$ EA values, leading to lower yields. A plausible mechanism for the intramolecular reaction would involve the initial formation of aryl radicals and subsequent photoinduced base-promoted homolytic aromatic substitution reaction (photo-BHAS).

Scheidt and colleagues extended the scope of photocatalyzed C–H activation by developing a photocatalytic variant of the Oxa-Pictet–Spengler reaction, a classic method for chromene synthesis.<sup>[19]</sup> Using benzylic ether substrates bearing an additional nucleophilic aryl group, the process selectively introduces a benzoate functional group at the  $\alpha$ -position of the ether. This transformation, induced by photocatalyst  $[\text{Ir}(\text{dF}(\text{CF}_3)\text{ppy})_2(\text{dtbbpy})](\text{PF}_6)$  (**PC3**), generates a benzoate acetal key intermediate which, upon treatment with a Lewis acid catalyst, forms an oxocarbenium species that undergoes ring closure to yield the isochromane product (Scheme 7).

Thus, when 1-[2-(aryloxy)ethyl]-methoxybenzene was treated with **PC3**, benzoyl peroxide ( $\text{BzO}_2$ ), and 1-butanethiol, under blue LED irradiation, followed by bismuth triflate-mediated Oxa-Pictet–Spengler reaction, in dichloroethane (DCE), the corresponding isochromane products were obtained (16 examples, 26–83%). The proposed mechanism initially involves the reduction of benzoylperoxide by the excited photocatalyst to provide benzoate radical. The oxidized photocatalyst can then generate a thiyl radical, which selectively abstracts a hydrogen atom at the benzylic position of the benzyl-ether substrates to furnish radical species **13**. Radical–radical cross-coupling between **13** and the benzoate radical provides key intermediate **14**. Then, bismuth-mediated elimination of the benzoate group of **14** affords oxocarbenium ion **15**, which undergoes an Oxa-Pictet–Spengler reaction to deliver the final product (Scheme 7).



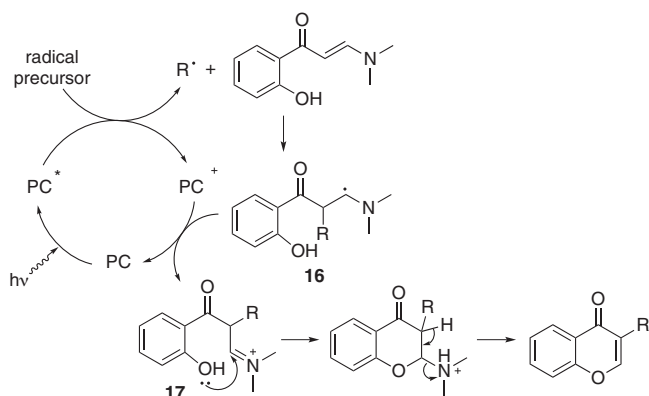
**Scheme 7.** Combination of photocatalysis and oxa-Pictet–Spengler reaction for the synthesis of isochromanes and proposed mechanism. “Reprinted (adapted) with permission from American Chemical Society. Copyright (2025).”

## 2.2. Synthesis of Chromenones

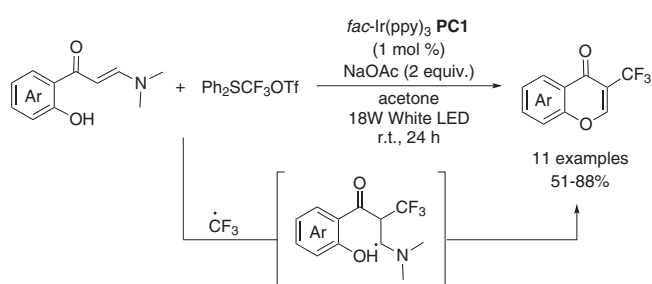
### 2.2.1. Synthesis of 4H-Chromenones (Chromones)

The chromone motif is the central moiety in numerous natural products, including flavonoids and isoflavonoids.<sup>[20]</sup> In the past few years, chromones have emerged as privileged heterocyclic scaffolds in drug discovery due to their diverse and promising biological activities.<sup>[21]</sup> On account of their relevance in both chemistry and biology, the synthesis of chromone derivatives has become a subject of great interest.<sup>[22]</sup> In particular, those bearing substituents at the C-3 position have drawn considerable attention as they exhibit a variety of physiological and biological properties.<sup>[23]</sup> Accordingly, developing efficient synthetic methodologies for these derivatives remains a highly active area of study. Among these approaches, those based on the tandem C–H elaboration combined with chromone annulation of *o*-hydroxyaryl enaminones stand out as one of the most widely adopted strategies.<sup>[24]</sup> In this regard, visible-light photoredox catalysis has also contributed to accessing a wide range of C3-substituted chromones under straightforward and environmentally friendly conditions from the corresponding *o*-hydroxyaryl enaminones.

The general mechanism for these types of transformations involves the generation of the excited state of the photocatalyst under visible light irradiation, which then promotes the formation of radical species  $\text{R}^\bullet$  (Scheme 8). Subsequently, the radical attacks the enaminone  $\text{C}=\text{C}$  to give radical intermediate **16** that is then quickly oxidized to form iminium intermediate



**Scheme 8.** General mechanism for the photocatalyzed synthesis of 3-C-substituted chromones.

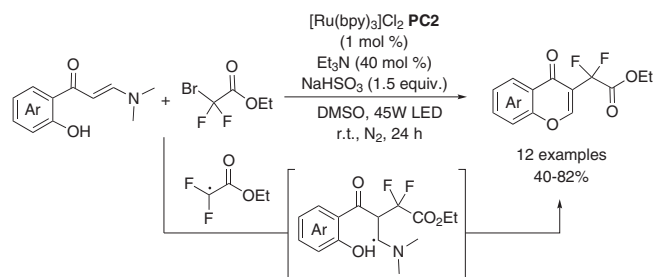


**Scheme 9.** Photocatalyzed synthesis of 3-CF<sub>3</sub>-substituted chromones from *o*-hydroxyaryl enaminones.

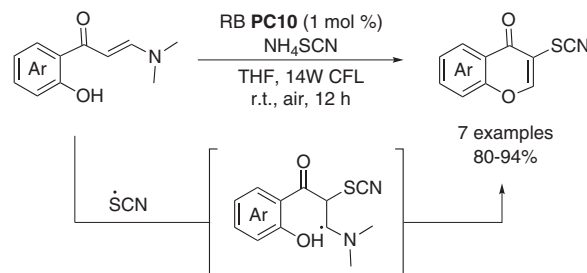
17 with the concurrent regeneration of the ground state of the photocatalyst. Finally, cyclization of the iminium intermediate followed by elimination of the *N,N*-dialkyl group furnish the desired 3-C-functionalized chromones.

The first application of this light-driven strategy for chromone synthesis was reported by Xiang et al. in 2017.<sup>[25]</sup> In their study, the authors combined their interest in chromone fluorination with previous reports on the photocatalytic generation of CF<sub>2</sub> and CF<sub>3</sub> radicals from Langlois/Togni/Umemoto reagents<sup>[26]</sup> to develop a visible-light-induced synthesis of 3-CF<sub>2</sub>/CF<sub>3</sub>-containing chromones. In contrast to earlier approaches, this photoredox process proceeds under mild conditions, avoiding heating and the use of inert atmosphere. The reaction of *o*-hydroxyaryl enaminones with Ph<sub>2</sub>SCF<sub>3</sub>OTf as the CF<sub>3</sub> source in the presence of *fac*-Ir(ppy)<sub>3</sub> catalyst (**PC1**) and white LED irradiation gave 3-CF<sub>3</sub>-substituted chromones in good yields (11 examples, 51–88%, Scheme 9). Diverse functional groups were well tolerated; however, the introduction of a halogen substituent at the *para*-position of the *o*-hydroxyaryl moiety led to a significant decrease in the corresponding yields.

In the same year, Zhang and co-workers described the preparation of 3-CF<sub>2</sub>-containing chromones via the photocatalytic radical cascade reaction of *o*-hydroxyaryl enaminones and ethyl bromodifluoroacetate in the presence of Et<sub>3</sub>N as reducing agent, NaHSO<sub>3</sub> as base and ruthenium-based catalyst **PC2**. Under these conditions, the corresponding chromones were obtained from moderate to good yields (12 examples, 40–82%, Scheme 10).<sup>[27]</sup>



**Scheme 10.** Photocatalyzed synthesis of 3-CF<sub>2</sub>-containing chromones from *o*-hydroxyaryl enaminones.



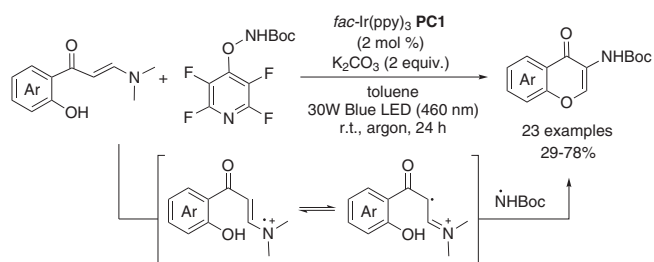
**Scheme 11.** Synthesis of 3-thiocyanated chromones from *o*-hydroxyaryl enaminones.

The reaction proceeds successfully with both electron-withdrawing and electron-donating groups on the aromatic ring of the enaminone. However, the yield is significantly affected by the position of the substituent. Substrates bearing methyl, methoxy, or fluoro groups at the *ortho*- or *para*-positions to the keto group gave the corresponding 3-CF<sub>2</sub>-containing chromones in good yields, while the identical substituents at the *meta*-position resulted in only moderate yields.

Expanding upon the synthesis of C3-functionalized chromones, Wan and co-workers successfully constructed the chromone ring from *o*-hydroxyaryl enaminones with concomitant insertion of a thiocyanate group at the C-3 position. Thus, visible-light irradiation (14W CFL) of *o*-hydroxyaryl enaminones in the presence of ammonium thiocyanate and only 1.0 mol% loading of non-metal photocatalyst Rose Bengal (**PC10**) afforded the expected 3-thiocyanated chromones in excellent yields (7 examples, 80–94%, Scheme 11).<sup>[28]</sup> The reaction accommodated enaminone substrates containing both electron-donating and electron-withdrawing groups.

Unlike other types of C3-functionalized chromones and despite their biological relevance, there are limited reports on the synthesis of C3-amino substituted analogs. In addition, the methodologies based on classical two-electron chemistry usually involve multiple steps and toxic reagents. Building on previous photocatalytic approaches for accessing 3-functionalized chromones, Wang et al. reported the first photocatalyzed strategy for the preparation of 3-aminochromones.<sup>[29]</sup> For this purpose, they employed the amidyl-radical precursor *tert*-butyl [(perfluoropyridin-4-yl)oxy]carbamate as amination reagent in the presence of a base and iridium photocatalyst **PC1**, under blue LED irradiation to achieve the corresponding products from moderate to good yields (23 examples, 29–78%, Scheme 12).



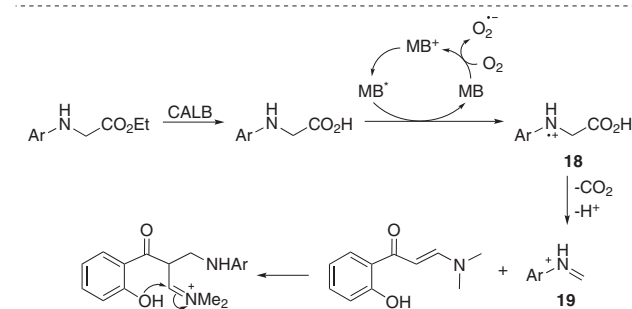
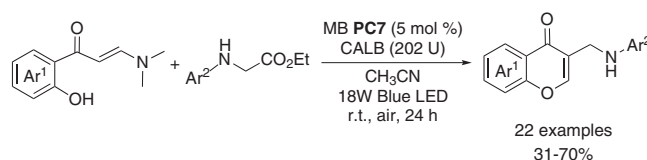


**Scheme 12.** Photocatalytic cascade for the preparation of 3-aminochromones.

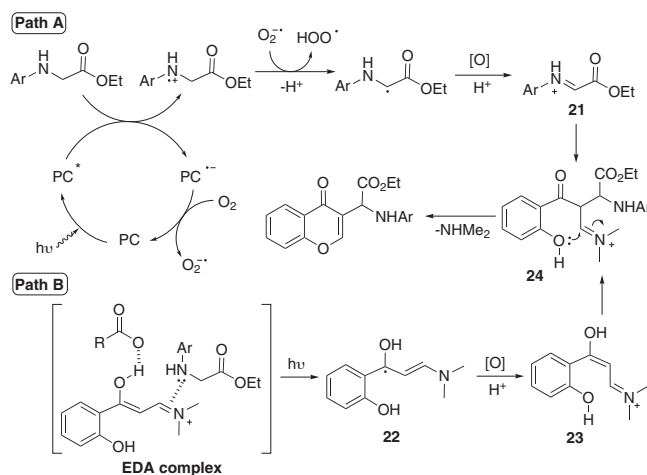
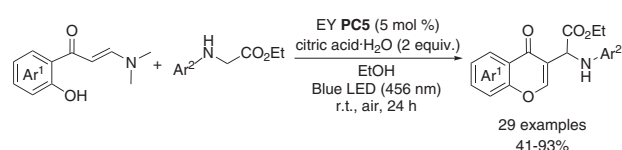
Regarding the scope of this phototransformation, halo-genated groups on the phenol moiety were well tolerated, but the reaction failed with strong electron-donating methoxy group. The efficacy of the process is also slightly affected by the position of the substituents on the phenol ring. Substrates with *para*-substituted phenol groups generally gave higher yields than their *meta*-substituted counterparts. Disubstituted *o*-hydroxyarylenaminones also successfully delivered the corresponding 3-aminochromones, albeit with lower yield in most cases.

Photoenzymatic reactions, which integrate both light and enzymes to facilitate the formation of chemical bonds, have recently become a new synthetic tool to attain chemical diversity.<sup>[30]</sup> In this sense, Hu et al. reported a practical and efficient strategy for the synthesis of C3-functionalized chromones combining photoredox and enzyme catalysis.<sup>[31]</sup> Thus, reaction of *o*-hydroxyaryl enaminones and different *N*-arylglycines in the presence of both *Candida antarctica* Lipase B (CAL-B) and Methylene Blue (PC7) enabled the synthesis of C3-substituted chromones featuring an  $\alpha$ -amino acid residue in moderate to good yields (22 examples, 31–70%, Scheme 13). *N*-arylglycine esters bearing electron-donating groups at the *para*-position of the aryl ring gave the best results. The proposed mechanism begins with the hydrolysis of *N*-arylglycine ester into *N*-arylglycine in the presence of CAL-B. Then, the excited photocatalyst formed under visible-light irradiation promotes the single electron transfer (SET) oxidation of *N*-arylglycine to form radical cation **18**. Subsequent deprotonation, decarboxylation, and oxidation give iminium intermediate **19**, which then reacts with *o*-hydroxyphenyl enaminone to generate iminium intermediate **20**. Intramolecular nucleophilic cyclization and elimination of dimethylamine finally afford the desired 3-substituted chromone (Scheme 13).

Cross-dehydrogenative coupling (CDC) reactions are highly valuable for forging new chemical bonds as they bypass functional group interconversions while offering atom economy and environmental benefits.<sup>[32]</sup> The CDC of *o*-hydroxyarylenaminones followed by chromone cyclization provides an efficient route to C3-alkylchromones. However, this process is challenging using traditional methods, with limited examples reported in the literature.<sup>[33]</sup> To address this challenge, Zhu et al. introduced an organophotocatalytic cascade CDC-coupling/cyclization between *o*-hydroxyaryl enaminones and *N*-arylglycine esters in the presence of Eosin Y (PC5) and hydrated citric acid under blue LED irradiation and an open-air atmosphere. Under these

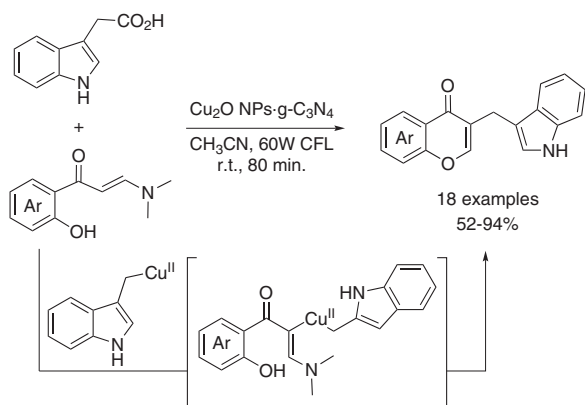


**Scheme 13.** Photoenzymatic synthesis of 3-aminoalkyl chromones and proposed mechanism. "Reprinted (adapted) with permission from American Chemical Society. Copyright {2025}."



**Scheme 14.** Visible-light-enabled cascade cross-dehydrogenative-coupling/cyclization of *o*-hydroxyaryl enaminones with glycine derivatives and proposed mechanism. "Used with permission of [Royal Society of Chemistry]. Order license ID 1585471-1/2025."

conditions, the corresponding coupled cyclization products were obtained from moderate to good yields (29 examples, 41–93%, Scheme 14).<sup>[34]</sup> The methodology tolerates a wide array of *o*-hydroxyarylenaminones and *N*-arylglycine esters. In general terms, enaminones bearing electron-withdrawing groups on the benzene rings were more favorable for the transformation than

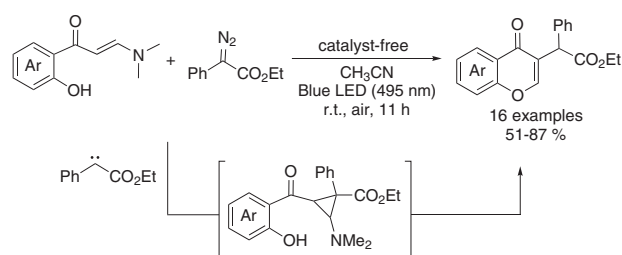


Scheme 15. Visible-light-mediated synthesis of 3-indolmethyl chromones.

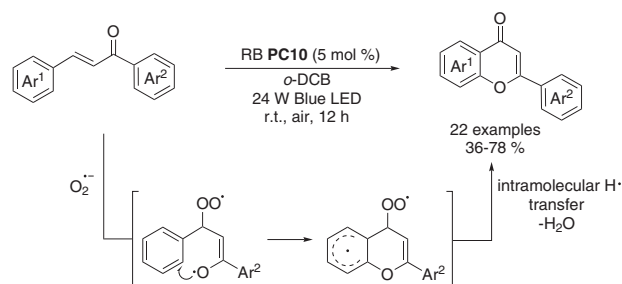
those bearing electron-donating groups. A plausible mechanism begins with the excitation of the photocatalyst Eosin Y\* (PC5) upon irradiation, followed by a single electron transfer (SET) with *N*-4-methylphenylglycine ester to afford the corresponding radical cation. Meanwhile, Eosin Y radical cation is oxidized by molecular oxygen, regenerating the ground-state Eosin Y and superoxide radical anion ( $O_2^{\bullet-}$ ), which then reacts with the radical cation intermediate to furnish an aminoalkyl radical. In the presence of citric acid, the radical is oxidized to the corresponding iminium **21** (path A). On the other hand, irradiation of the ternary-colored EDA complex formed by the enaminone, the amine and the citric acid afforded radical intermediate **22**, which was then oxidized to **23** (path B). Reaction of **21** and **23** gave key intermediate **24**, which finally underwent intramolecular nucleophilic cyclization and elimination of dimethylamine to deliver the desired product (Scheme 14).

Another example of a light-based, eco-friendly synthesis of 3-alkylated chromones from *o*-hydroxyaryl enaminones was described by Talpada et al. in 2024.<sup>[35]</sup> This study describes the cyclization/alkylation reaction of *o*-hydroxyaryl enaminones with 3-indoleacetic acid in the presence of copper nanoparticles ( $Cu_2O$  NPs) supported on graphitic carbon nitride ( $g-C_3N_4$ ), under visible-light, to afford 3-indolmethyl chromones from moderate to excellent yields (18 examples, 52–94%, Scheme 15). Notably, the heterogeneous catalyst can be reused for up to five cycles without significantly decreasing activity. Regarding the reaction scope, *o*-hydroxyaryl enaminones bearing electron-donating groups afforded desired alkylated products from good to excellent yields (74–94%). In contrast, enaminones bearing strongly electron-withdrawing nitro groups showed lower efficiency (52–61% yields). Mechanistically, the reaction initiates with the interaction between 3-indoleacetic acids and  $Cu_2O$  NPs- $g-C_3N_4$ , under the irradiation of visible light, resulting in the formation of a copper carboxylate. This carboxylate subsequently loses  $CO_2$ , forming the corresponding organocopper compound, which then reacts with the enaminone. Reductive elimination from the resulting organocopper intermediate, followed by removal of the dimethylamine, furnished desired 3-indolmethyl chromones.

The methods discussed so far for synthesizing C3-substituted chromones require the use of catalysts and additives, which inevitably increases the cost and may limit their practical applica-



Scheme 16. Visible-light-induced synthesis of 3-alkylchromones under catalyst- and additive-free conditions.

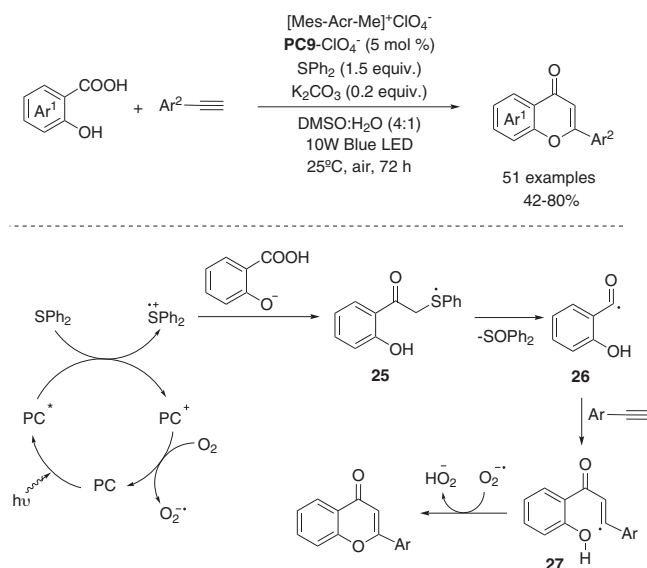


Scheme 17. Visible-light-induced C(sp<sup>2</sup>)-H functionalization/C–O bond formation.

tions. Thus, developing green and efficient chromone synthetic methodologies that operate without catalysts and additives under mild conditions remains highly desirable. In this regard, Zhao et al. introduced a visible-light-induced procedure for synthesizing 3-alkylchromones from *o*-hydroxyaryl enaminones and  $\alpha$ -diazo ester.<sup>[36]</sup> This protocol is based on the reaction of *o*-hydroxyaryl enaminones and carbene precursors generated from diazo compounds under visible-light, eliminating the need for catalysts and producing only non-toxic  $N_2$  as the sole by-product. Treatment of *o*-hydroxyphenyl enaminones with ethyl 2-diazo-2-arylacetates under blue LED irradiation at room temperature afforded desired 3-alkylchromones from moderate to high yields (16 examples, 51–87%, Scheme 16). This alkylation reaction showed good tolerance for both electron-donating and electron-withdrawing substituents on the aromatic ring of the diazo compounds. Additionally, enaminones bearing electron-withdrawing and electron-donating groups at different positions of the aromatic ring also gave satisfactory results.

Flavones (2-phenyl-4*H*-chromen-4-ones) are an essential class of chromene derivatives prevalent in the vegetal kingdom, known for their diverse biological and pharmacological activities.<sup>[37]</sup> Several visible-light-mediated strategies have been developed to prepare these relevant chromene derivatives.

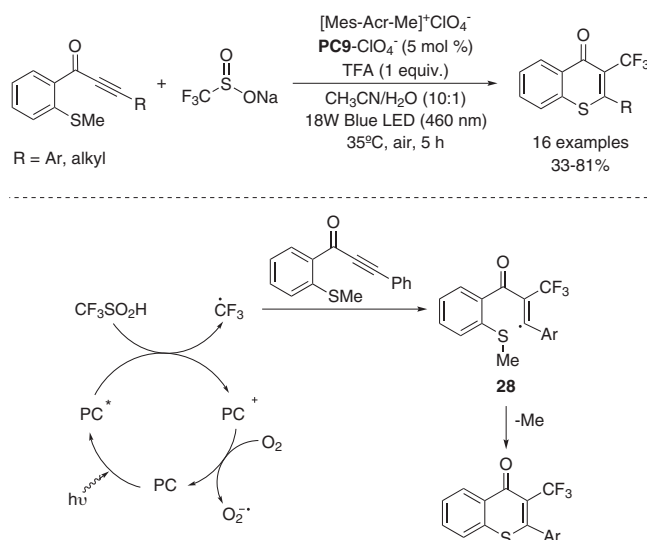
For example, Lin and co-workers reported the synthesis of flavones from chalcones (1,3-diphenylprop-2-en-1-ones) based on the visible-light-induced C(sp<sup>2</sup>)-H functionalization/C–O bond formation (Scheme 17).<sup>[38]</sup> This reaction utilizes the organic dye Rose Bengal (PC10) as the photosensitizer and atmospheric oxygen as both oxidant and oxygen source, not requiring the presence of any metals or external additives. Through this protocol, a variety of flavones were synthesized from moderate to good yields (22 examples, 36–78%). Generally, chalcones bearing



**Scheme 18.** Photocatalytic deoxygenative/cyclization reaction of salicylic acid derivatives with aryl acetylenes and proposed mechanism. “Used with permission of [Royal Society of Chemistry]. Order license ID 1585472-1/2025”.

electron-donating substituents reacted faster than those with electron-withdrawing ones but with a minor effect on the final yields. Nevertheless, steric factors had a significant impact on the reaction efficiency, as shifting the substituent from the *para*-position to the *meta*- or *ortho*-position resulted in a notable decrease in yield. This photo-oxygenation process is initiated by the reaction of the chalcone and singlet oxygen, generated under photocatalytic conditions. The resulting oxo radical attacks the benzene ring to form a radical intermediate, which on subsequent intramolecular H transfer followed by elimination of H<sub>2</sub>O provides the corresponding flavones.

Chu and colleagues described the preparation of flavones through a visible-light-induced deoxygenative/cyclization reaction of salicylic acid derivatives with aryl acetylenes using diphenyl sulfide as an *O*-transfer reagent.<sup>[39]</sup> Thus, reaction of salicylic acids and arylacetylenes in the presence of [Mes-Acr-Me]<sup>+</sup>ClO<sub>4</sub><sup>−</sup> (PC9-ClO<sub>4</sub><sup>−</sup>), as photocatalyst, SPh<sub>2</sub>, and K<sub>2</sub>CO<sub>3</sub>, under blue LED irradiation, afforded flavones from moderate to good yields (51 examples, 42–80%, Scheme 18). The reaction is applicable to a wide range of arylacetylenes and salicylic acids with various substituents, with electron-donating groups providing comparatively higher yields than electron-withdrawing groups. To further showcase the practicality of this approach, a series of natural flavones featuring multiple hydroxyl and methoxy groups were also successfully synthesized. Regarding the proposed mechanism, the process is initiated by the generation of the excited photocatalyst under irradiation of blue light. The photoexcited catalyst undergoes SET oxidation with SPh<sub>2</sub> to form the diphenyl sulfide radical cation, which subsequently reacts with carboxylate anions to generate radical **25**. Next, radical **25** undergoes C–O bond cleavage to generate acyl radical **26**, which upon reaction with arylacetylene provides radical species **27**. The reduced photocatalyst is oxidized by the residual oxygen to regenerate the ground state and form anion radical (O<sub>2</sub><sup>•−</sup>),

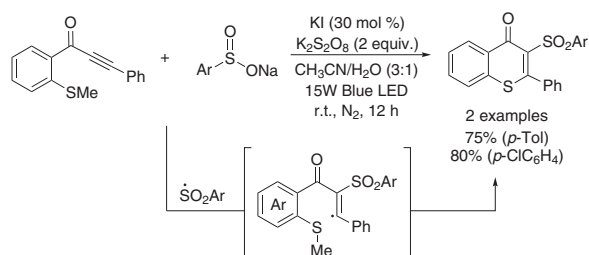


**Scheme 19.** Visible-light-promoted perfluoroalkylation/cyclization for the construction of perfluoroalkylated thioflavones, along with the mechanistic proposal.

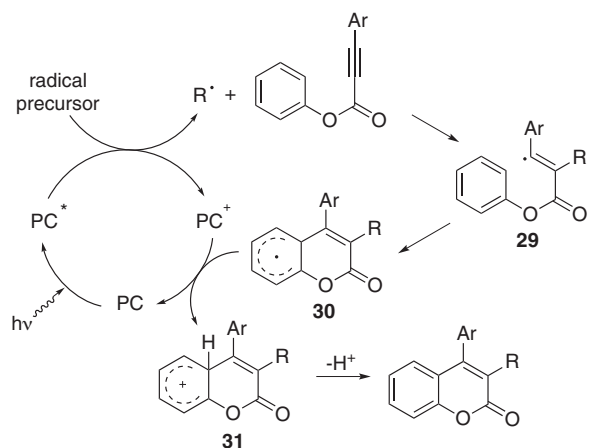
which then abstracted a hydrogen atom from **27** to finally furnish the desired flavone derivatives (Scheme 18).

Ma et al. reported a visible-light-promoted transition-metal-free perfluoroalkylation/cyclization for the synthesis of 3-perfluoroalkylated thioflavones.<sup>[40]</sup> By reacting methylthiolated alkynes and CF<sub>3</sub>SO<sub>2</sub>Na in the presence of [Mes-Acr-Me]<sup>+</sup>ClO<sub>4</sub><sup>−</sup> (PC9-ClO<sub>4</sub><sup>−</sup>) as the photocatalyst and trifluoroacetic acid (TFA) as the acid additive under blue LED irradiation at 35 °C, they achieved the target perfluoroalkylated thioflavones from moderate to good yields (16 examples, 33–81%, Scheme 19). This radical-based strategy demonstrates broad tolerance toward both electron-rich and electron-deficient methylthiolated alkynes. Notably, among the synthesized 3-perfluoroalkylated compounds, 4'-cyano thioflavone exhibited significant anti-tumor activity, emerging as a promising lead for developing novel drugs for the clinical treatment of human lymphoma and cervical carcinoma. The mechanism for this transformation involves the formation of the trifluoromethyl radical on reaction of trifluoromethanesulfonic acid with the excited state of the photocatalyst, subsequent reaction with the methylthiolated alkynes to generate radical intermediate **28** and cyclization/demethylation to finally afford desired thioflavones (Scheme 19).

Building on the work of Ma et al., Dong and co-workers also reported a photoinduced radical cascade cyclization of methylthiolated alkynes with sodium sulfinates, enabling the divergent synthesis of sulfonated thioflavones under metal- and photocatalyst-free conditions.<sup>[41]</sup> Reaction of methylthiolated alkynes and sodium *p*-tolyl- or *p*-chlorobenzenesulfinate in the presence of KI as an additive, and K<sub>2</sub>S<sub>2</sub>O<sub>8</sub> as an oxidant, under blue LED light, gave the corresponding 3-sulfonyl thioflavones in good yields (2 examples, 75–80%, Scheme 20). In this process, the required sulfonyl radical was generated directly from the excited state of I<sub>2</sub><sup>\*</sup>, produced upon visible-light irradiation of I<sub>2</sub>, formed in situ by oxidation of KI with K<sub>2</sub>S<sub>2</sub>O<sub>8</sub>.



**Scheme 20.** Photoinduced cascade cyclization of alkynes with sodium sulfinates for the synthesis of thioflavones.

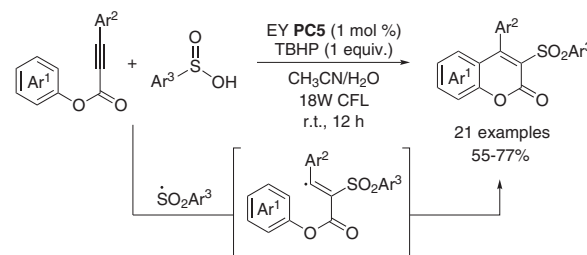


**Scheme 21.** General mechanism for the visible-light-induced cascade radical addition/cyclization.

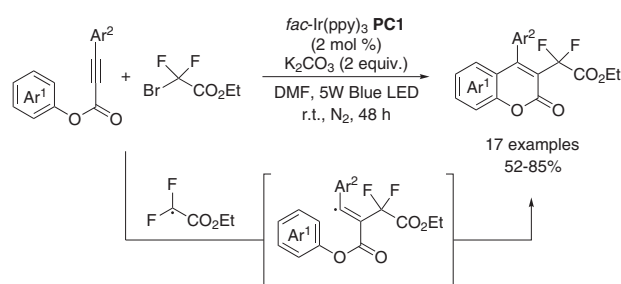
### 2.2.2. Synthesis of 2H-chromenones (coumarins)

The coumarin skeleton is omnipresent in the structure of bioactive natural products, pharmaceuticals, agrochemicals, and functional materials.<sup>[42]</sup> Consequently, the development of simple and efficient methods for the preparation of coumarins has attracted considerable attention.<sup>[43]</sup> Many of these methods traditionally relied on transition-metal-catalyzed cyclizations, particularly in recent decades.<sup>[44]</sup> However, the requirement of toxic metals, ligands, or additives limits their applications in the pharmaceutical industry. Over the past decade, visible-light-induced radical-involved cyclization reactions have been established as a more convenient and greener alternative for synthesizing functionalized coumarins under mild conditions.

**From Alkynes:** Aryl alkynoates, owing to their ease of preparation and susceptibility toward radical addition, have been extensively used as radical acceptors in a range of visible-light-mediated cyclizations to access substituted coumarins. The general mechanism for these transformations, which involve the domino radical addition/cyclization reaction of aryl alkynoates, is depicted in Scheme 21. The process begins with the generation of radical species through a single-electron transfer (SET) between the excited state of the photocatalyst and a radical precursor. Then, radical addition to aryl alkynoate forms radical intermediate **29**, which cyclizes to radical **30** and is then further transformed into carbocation intermediate **31** through oxidation



**Scheme 22.** Visible-light-initiated oxidative cyclization of aryl propiolates with sulfinic acids to coumarin derivatives.



**Scheme 23.** Visible-light-mediated synthesis of 3-difluoroacetylated coumarins.

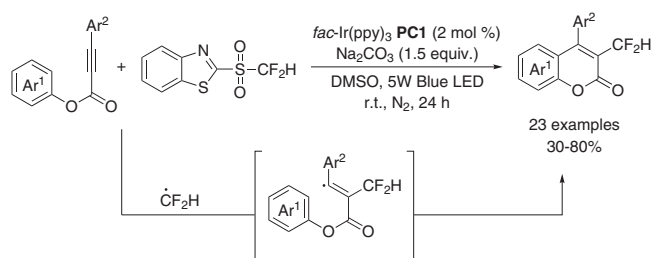
by the radical cation of the photocatalyst. Finally, carbocation **31** is deprotonated, regenerating the aromatic system and affording the desired 3-substituted coumarin product.

There are several examples in the literature of the application of this strategy to the synthesis of substituted coumarins. For instance, Wang and co-workers developed the visible-light-initiated oxidative cyclization of aryl propiolates with sulfinic acids to generate sulfonylated coumarin derivatives.<sup>[45]</sup> Thus, reaction of 3-arylpropiolates and arenesulfinic acids in the presence of organic photocatalyst Eosin Y (PC5) and *tert*-butyl hydroperoxide (TBHP) as oxidant, under irradiation of an 18 W CFL afforded 3-sulfonyl coumarins with wide functional group tolerance, good yields and high regioselectivities (21 examples, Scheme 22).

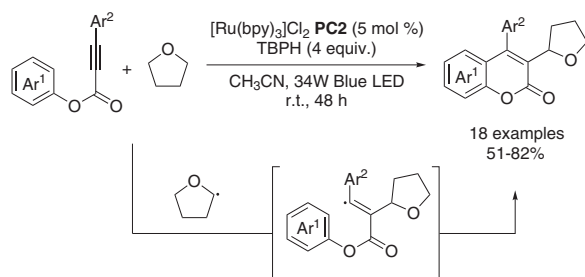
The arylsulfonylations of aryl propiolates containing electron-donating groups or halogen atoms at the *para*- and *meta*-positions of the phenyl rings provided the corresponding coumarins from moderate to good yields (55–77%). However, a significant steric effect was observed, as *ortho*-substituted aryl propiolates yielded only trace amounts of the desired products.

The photocatalyzed domino radical addition/cyclization of aryl alkynoates has also proven to be a suitable strategy for furnishing alkylated coumarins. For example, Fu et al. reported the synthesis of 3-difluoroacetylated coumarins.<sup>[46]</sup> In this process, aryl alkynoates reacted with ethyl bromodifluoroacetate in the presence of iridium photocatalyst *fac*-Ir(ppy)<sub>3</sub> (PC1) and K<sub>2</sub>CO<sub>3</sub> under blue LED irradiation to obtain 3-difluoroacetylated coumarins from modest to good yields (17 examples, 52–85%, Scheme 23). Both moderate electron-withdrawing groups and electron-donating groups at the *para*-position of the aryl 3-phenylpropiolates were well tolerated. In contrast, *meta*-substituted substrates gave mixtures of regioisomers with





Scheme 24. Visible-light-mediated direct difluoromethylation of alkynoates.



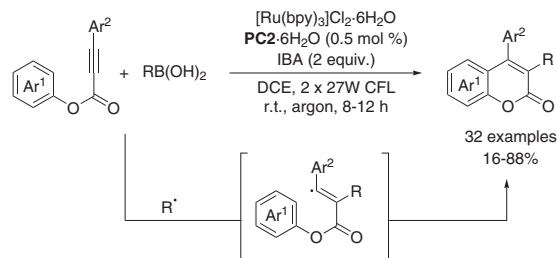
Scheme 25. Visible-light-promoted domino radical addition/cyclization reaction for the synthesis of 3-etherified coumarins.

moderate selectivity, while *ortho*-substituted counterparts did not yield any product due to steric hindrance.

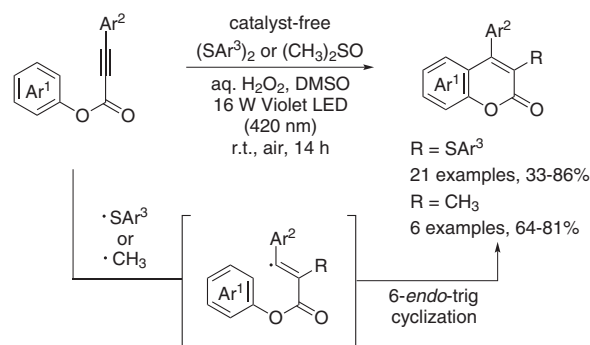
In a subsequent study, the same researchers demonstrated the usefulness of this visible-light-induced cyclization/alkylation of aryl alkynoates by synthesizing 3-difluoromethylated coumarins via a radical-triggered cascade difluoromethylation/cyclization migration of alkynoates.<sup>[47]</sup> Thus, aryl alkynoates reacted with benzo[d]thiazole difluoromethyl sulfone, serving as a CF<sub>2</sub>H radical source, in the presence of *fac*-Ir(ppy)<sub>3</sub> (PC1) as the photocatalyst, under blue LED irradiation, giving the desired products from moderate to high yields (23 examples, 30–80%, Scheme 24). Substrates bearing electron-donating or electron-withdrawing groups at the *para*-position of the aryl 3-phenylpropiolates performed well. However, *meta*-substituted substrates provided mixtures of regioisomers, and once again, strong steric effect prevented *ortho*-substituted alkynoates from undergoing the reaction.

Following a similar domino radical addition/cyclization approach, She and co-workers reported the preparation of 3-etherified coumarins.<sup>[48]</sup> The reaction of aryl 3-arylpropiolates with tetrahydrofuran (THF) in the presence of TBHP as oxidant, using a blue LED strip as the light source and [Ru(bpy)<sub>3</sub>]Cl<sub>2</sub> (PC2) as photocatalyst afforded desired 3-etherified coumarins from moderate to good yields (18 examples, 51–82%, Scheme 25). The reaction accommodates alkynoates containing alkyl and halogen substituents in *para*- and *meta*-position. However, strong electron-donating methoxy group was unsuitable under the reaction conditions. Moreover, a significant steric effect was observed for *ortho*-substituted alkynoates, which provided only trace amounts of the desired coumarin products.

More recently, Prabhu and co-workers used organoboronic acids in the cascade alkylation/cyclization of aryl alkynoates to synthesize 3-alkylated coumarins.<sup>[49]</sup> The reaction of aryl



Scheme 26. Visible-light-mediated reaction of arylalkynoates with boronic acids.



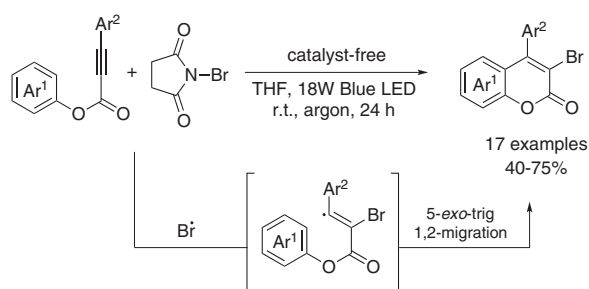
Scheme 27. Photocatalyst-free synthesis of coumarins from aryl alkynoates.

alkynoates and alkyl boronic acids in the presence of hypervalent iodine oxidant 2-iodosobenzoic acid (IBA), and a hydrated ruthenium photocatalyst [Ru(bpy)<sub>3</sub>]Cl<sub>2</sub>·6H<sub>2</sub>O (PC2·6H<sub>2</sub>O) afforded 3-alkylated coumarins, under visible-light irradiation (32 examples, 16–88%, Scheme 26).

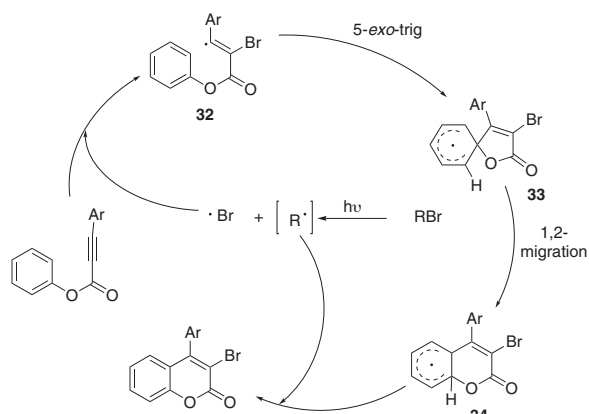
In 2024, Natarajan et al. introduced an eco-friendly and novel methodology for synthesizing 3-substituted coumarins through selective tandem cyclization of aryl alkynoate esters under violet LED irradiation (Scheme 27).<sup>[50]</sup> This metal-, catalyst-, additive-free protocol operates under mild conditions and uses a non-toxic solvent, aligning with green chemistry principles. The methodology tolerates a broad substrate scope, delivering 3-sulfonylcoumarins (21 examples) or 3-methylcoumarins (6 examples) from moderate to good yields upon treatment with a suitable sulfonylation or alkylation agent, respectively. Thus, addition of either aryl sulfonyl [ $\bullet$ SAr<sup>3</sup>] or methyl radical [ $\bullet$ CH<sub>3</sub>] to the aryl alkynoate ester produces a vinyl radical intermediate, which on intramolecular 6-*endo*-trig cyclization, oxidation and deprotonation furnish the intended 3-substituted coumarins.

Based on the potential of alkynoates as radical receptors and valuable intermediates for constructing 3-functionalized coumarins, Ding and coworkers developed a radical brominative addition of alkynoates for the synthesis of 3-bromocoumarins.<sup>[51]</sup>

It is well known that the bromo group certainly occupies a pivotal position in organic synthesis, particularly owing to its versatility as building block in transition-metal-catalyzed coupling reactions,<sup>[52]</sup> therefore significant efforts have been dedicated to incorporating bromo into the coumarin backbone.<sup>[53]</sup> Nevertheless, Ding's approach relied on traditional methods for generating the bromo radical, which required high reaction



**Scheme 28.** Photocatalyst-free synthesis of 3-bromocoumarins from aryl alkynoates.



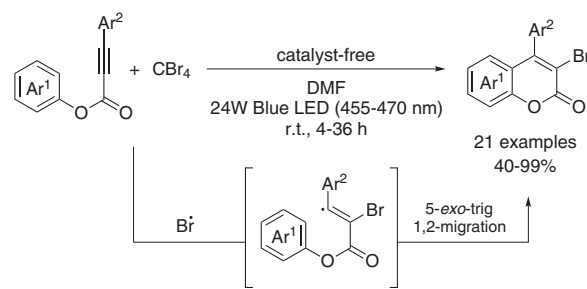
**Scheme 29.** Mechanism for the bromo radical addition/spiro-cyclization/ester migration cascade of aryl alkynoates.

temperatures and strong oxidants, limiting its practicality for large-scale applications involving complex bioactive compounds.

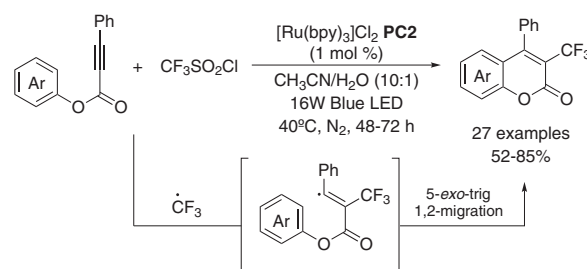
Stemming from Ding's group studies, She and colleagues reported a visible-light-mediated radical addition of alkynoates to generate 3-bromocoumarins by using *N*-bromosuccinimide (NBS) as bromine source.<sup>[54]</sup> Thus, the reaction of aryl alkynoates with NBS exposed to blue LED irradiation at room temperature yielded 3-bromocoumarins from moderate to good yields (17 examples, 40–75%), accommodating a broad range of alkynoate substrates (Scheme 28).

Similar to Ding's strategy, the process involves a bromo radical addition/spiro-cyclization/ester migration cascade reaction. However, the reaction proceeds under very mild conditions, without the need for a catalyst, strong oxidants, or elevated temperatures. In this case, the bromo radical is generated under the action of visible light. Subsequently, the selective addition of the bromo radical to the  $\alpha$ -position of the triple bond of aryl alkynoates generates a vinyl radical **32**. This radical undergoes an intramolecular 5-*exo*-trig spiro-cyclization, and a subsequent 1,2-migration of the resulting radical intermediate **33** leads to a radical intermediate **34**, which is then converted to the final product (Scheme 29).

A few years later, Yan et al. presented another approach for the synthesis of 3-bromocoumarins through a visible-light-induced tandem radical brominative addition/spiro-cyclization/1,2-ester migration of aryl alkynoates, this time employing  $\text{CBr}_4$  as the bromine radical source.<sup>[55]</sup> The reaction



**Scheme 30.** Photocatalyst-free synthesis of 3-bromocoumarins from aryl alkynoates.

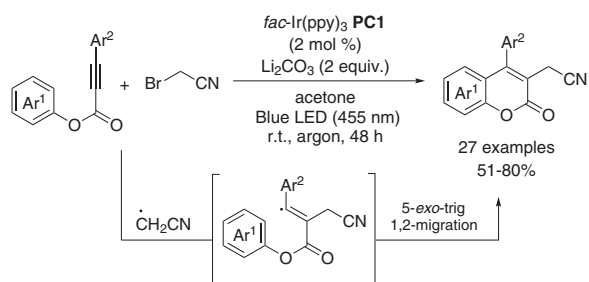


**Scheme 31.** Photoredox-catalyzed cascade radical cyclization of aryl propiolates for the synthesis of 3-trifluoromethyl coumarins.

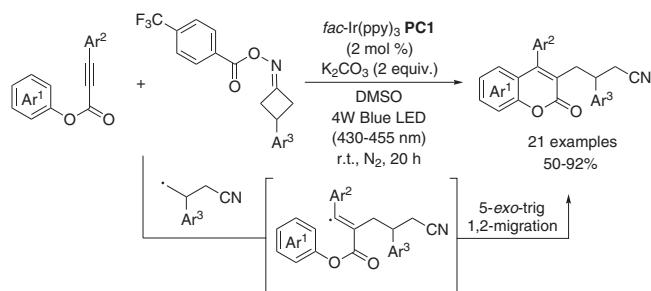
of aryl alkynoates with  $\text{CBr}_4$  under blue LED irradiation produced 3-bromocoumarins from moderate to quantitative yields (21 examples, 40–99%), showing a broad substrate scope and good functional group tolerance (Scheme 30).

Continuing with the synthesis of 3-halogenated coumarins by means of the visible-light-induced radical addition of alkynoates, Xiong and co-workers described the preparation of 3-fluorinated coumarin derivatives using  $\text{CF}_3\text{SO}_2\text{Cl}$  as the trifluoromethyl radical source.<sup>[56]</sup> Thus, reaction between aryl 3-phenylpropiolates and  $\text{CF}_3\text{SO}_2\text{Cl}$  was carried out under irradiation with a blue LED strip in the presence of  $[\text{Ru}(\text{bpy})_3]\text{Cl}_2$  (**PC2**) as the photocatalyst to afford 3-trifluoromethyl coumarins from moderate to good yields (27 examples, 52–85%, Scheme 31). The reaction demonstrated high efficiency and a broad substrate scope, tolerating aryl alkynoates with both electron-donating and electron-withdrawing substituents at the *para*- and *meta*-positions. Interestingly, substrates bearing a methyl group in *ortho*-position also afforded desired coumarins in moderate yields, indicating a subtle steric effect from the *ortho*-substitution.

The cascade radical addition/spiro-cyclization/1,2-ester migration of aryl alkynoates was also applied to the preparation of 3-alkyl and 3-acyl coumarins. For example, Zhang et al. reported the synthesis of 3-cyanomethylated coumarins by a visible-light-mediated cyanomethylation/spiro-cyclization of aryl alkynoates.<sup>[57]</sup> Thus, when reacting with aryl 3-arylpropiolate and bromoacetonitrile in the presence of *fac*- $\text{Ir}(\text{ppy})_3$  (**PC1**) as the photocatalyst and  $\text{Li}_2\text{CO}_3$  as a base, under blue-light irradiation, the desired 3-cyanomethyl coumarins were obtained from moderate to good yields (27 examples, 51–80% yields, Scheme 32). The process was effective regardless of the electronic properties or steric effects of the substituents on the aromatic ring attached to the alkyne moiety. However, the reaction did not occur when



**Scheme 32.** Visible-light-promoted synthesis of 3-cyanomethylated coumarins.



**Scheme 33.** Photocatalyzed radical cascade cyclization of acetylenic acid esters with oxime esters.

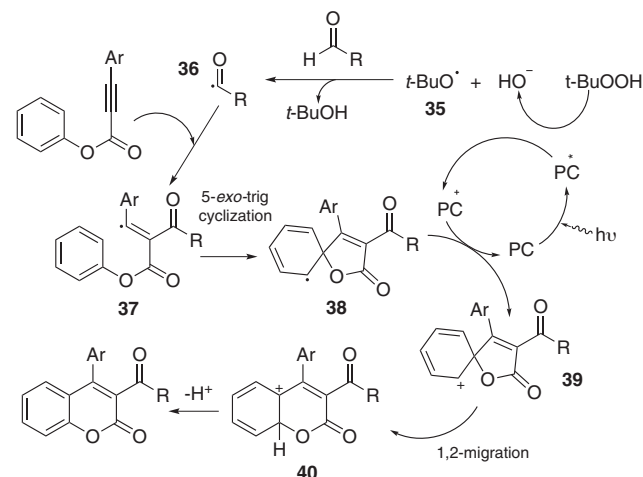
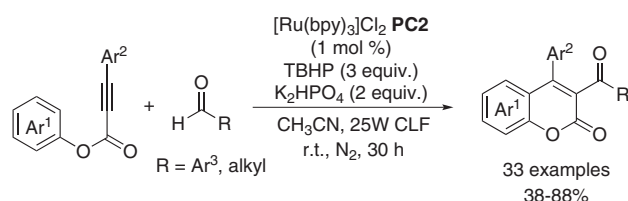
substrates with the substituents at the *ortho*-position of the phenoxy ring were used.

Later, in 2022, Yang et al. described another strategy for preparing cyanalkylated coumarins through the photoinduced radical cascade cyclization of acetylenic acid esters with oxime esters.<sup>[58]</sup> Thus, when aryl 3-arylpropiolates reacted with 3-phenylcyclobutan-1-one O-[4-(trifluoromethyl) benzoyl] oxime in the presence of *fac*-Ir(ppy)<sub>3</sub> (PC1) as the photocatalyst and K<sub>2</sub>CO<sub>3</sub> as a base, under blue-light irradiation, the desired 3-cyanoalkylated coumarins were achieved in moderate to excellent yields (21 examples, 50–92%, Scheme 33).

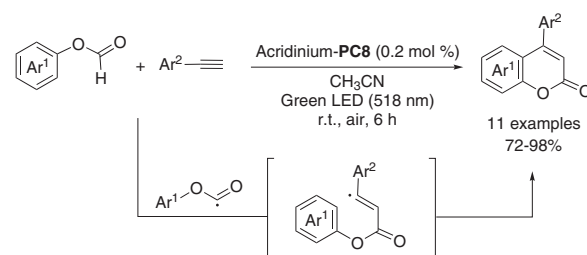
Jiang and co-workers developed the visible-light-promoted radical acylation/spiro-cyclization/1,2-ester migration method for synthesizing 3-acylcoumarins from alkynoates and aldehydes.<sup>[59]</sup> Starting from aryl alkynoates, the desired products were obtained from moderate to good yields (33 examples, 38–88%) upon treatment with aldehydes in the presence of [Ru(bpy)<sub>3</sub>]Cl<sub>2</sub>/TBHP (PC2/TBHP) as the photoredox catalyst/oxidant combination, K<sub>2</sub>HPO<sub>4</sub> as base and visible-light irradiation (Scheme 34).

The reaction is not only general for several linear alkyl aldehydes but also applicable to aromatic aldehydes. Regarding the scope of aryl alkynoates, both electron-donating groups and electron-withdrawing substituents were well tolerated.

The reaction begins with the generation of a *tert*-butoxy radical **35** through a single-electron transfer (SET) between the excited photocatalyst (PC\*) and TBHP. This radical then abstracts a hydrogen atom from the aldehyde, yielding the corresponding acyl radical **36** along with *tert*-butanol. Radical **36** subsequently adds to the aryl alkynoate, forming radical intermediate **37**, which undergoes an intramolecular 5-*exo*-trig cyclization, gener-



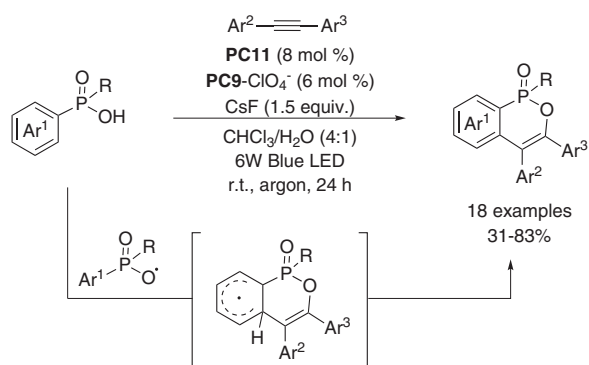
**Scheme 34.** Visible-light-promoted radical acylation/cyclization of aryl alkynoates with aldehydes for the synthesis of 3-acylcoumarins and proposed mechanism. "Used with permission of [Royal Society of Chemistry]. Order license ID 1585479-1/2025".



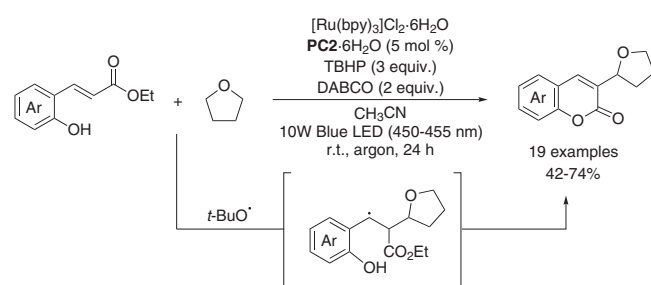
**Scheme 35.** Visible-light promotes synthesis of coumarins from aryl formates.

ating radical intermediate **38**. Oxidation of **38** by PC<sup>+</sup> produces cation **39**, which undergoes a 1,2-ester migration, leading to cation **40**. Ultimately, **40** is deprotonated in the presence of a base, restoring the aromatic system and yielding the desired 3-acylcoumarin products (Scheme 34).

In addition to the previously described cascade processes, Kashyap et al. reported an alternative strategy for the synthesis of coumarins, also employing alkynes as starting materials. This methodology involves the reaction between substituted ethynylarenes and aryl formates under green LED irradiation in the presence of acridinium photocatalyst PC8 and atmospheric oxygen as oxidant. Under these conditions, desired coumarin derivatives were obtained in good yields (11 examples, 72–98%, Scheme 35).<sup>[60]</sup> The reaction proceeds via a photoredox cycle where the photocatalyst, upon irradiation, oxidizes the aryl formate via SET, generating an acyl radical. This radical adds to the alkyne, forming a vinyl radical that undergoes subsequent



Scheme 36. Metallophotoredox synthesis of phosphaisocoumarins.

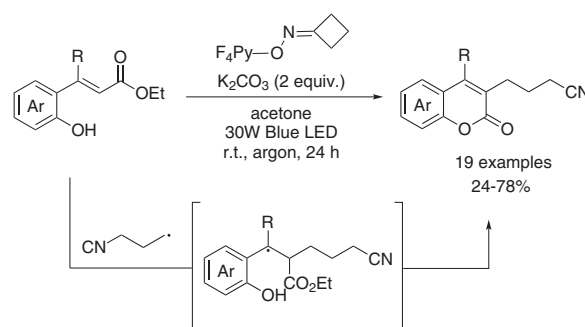
Scheme 37. Visible-light-induced C(sp<sup>2</sup>)–C(sp<sup>3</sup>) coupling reaction for the regioselective synthesis of 3-functionalized coumarins.

oxidative cyclization to yield the coumarin. Atmospheric oxygen facilitates catalyst regeneration and final oxidation.

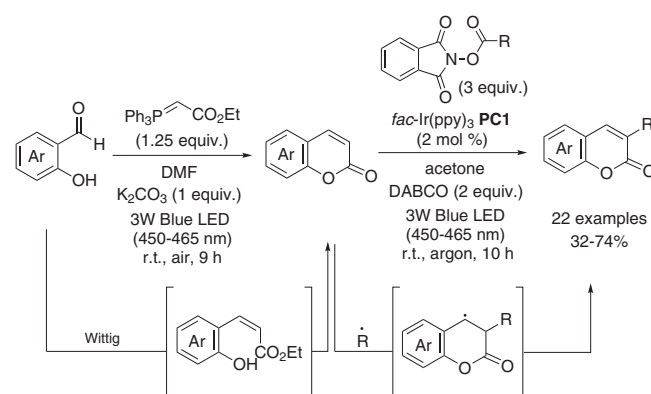
Shi and co-workers described an efficient and practical access to phosphaisocoumarins by using a dual catalytic system containing an acridinium photosensitizer and a cobaloxime proton-reducing catalyst ([Co(dmgH)<sub>2</sub>]PyCl) (**PC11**).<sup>[61]</sup> This visible-light-driven methodology involves the phosphinyloxy radical formation through O–H cleavage of arylphosphinic acids with H<sub>2</sub> release in the presence of a cobalt catalyst, followed by radical addition/cyclization with alkynes. Reaction of diarylphosphinic acids and diarylacetylene in the presence of [Mes-Acr-Me]<sup>+</sup>ClO<sub>4</sub><sup>−</sup> (**PC9-ClO<sub>4</sub><sup>−</sup>**) and [Co(dmgH)<sub>2</sub>]PyCl (**PC11**) as catalysts and CsF as base, under blue-light irradiation delivered the desired phosphaisocoumarins (Scheme 36).

Arylphosphinic acids bearing either electron-donating or electron-withdrawing groups on the benzene ring at various positions (ortho-, meta-, or para-) on the benzene ring were found to be suitable for the reaction, giving the corresponding products from moderate to good yields (18 examples, 31–83%).

**From alkenes:** The direct C–H functionalization through oxidative cross-coupling reactions of alkenes represents another powerful tool for synthesizing 3-substituted coumarins. In 2021, Zhang et al. introduced a photocatalytic strategy for the regioselective synthesis of 3-functionalized coumarins involving the alkenylation of the C(sp<sup>3</sup>)–H bond of ethers, followed by lactonization (Scheme 37).<sup>[62]</sup> The method offers a broad substrate scope and tolerates both electron-donating and electron-withdrawing groups at different positions of the phenol moiety, delivering 3-alkylated coumarins from moderate to good yields



Scheme 38. Visible-light-driven, photocatalyst-free cascade to access 3-cyanoalkyl coumarins.



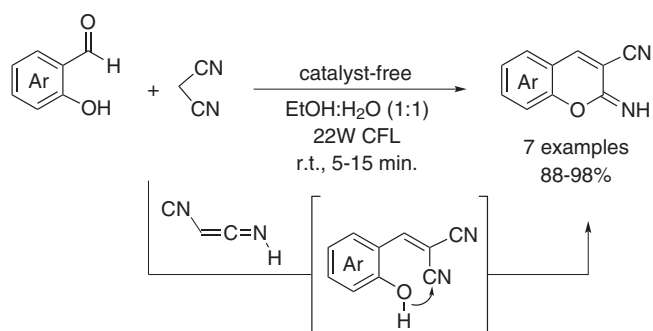
Scheme 39. Visible-light-induced synthesis of 3-alkylcoumarins from salicylaldehydes.

(19 examples, 42–74%). In this process, visible light irradiation of [Ru(bpy)<sub>3</sub>]Cl<sub>2</sub>·6H<sub>2</sub>O (**PC2·6H<sub>2</sub>O**) photocatalyst, promotes the formation of *t*-BuO• radical, which then abstracts a H atom from THF to furnish the corresponding carbon radical. Regioselective C(sp<sup>2</sup>)–C(sp<sup>3</sup>) coupling reaction with 3-(2-hydroxyaryl)acrylates affords an intermediate carbon radical, which undergoes deprotonation and lactonization to obtain 3-alkylated coumarins.

A similar strategy was employed by Hu et al. for the synthesis of 3-cyanoalkyl coumarins.<sup>[63]</sup> Their protocol involves a visible-light-driven, photocatalyst-free reaction of *o*-hydroxycinnamic esters and perfluoropyridin-4-yl oximes, enabling the rapid formation of a diverse array of 3-cyanoalkyl coumarins in the presence of K<sub>2</sub>CO<sub>3</sub> under blue LED irradiation (Scheme 38). Notably, no external photocatalyst is required, as the in situ generated phenolate anions act as photosensitizers to drive the photoinduced transformation. The protocol accommodates various substitution patterns on the aromatic rings of the esters, delivering the target products from moderate to good yields (19 examples, 24–78%).

**From Aldehydes:** 3-alkyl coumarins can also be prepared from inexpensive and readily available salicylaldehydes through a visible-light-induced one-pot Wittig/cyclic condensation/radical alkylation process, as described by Kim et al. (Scheme 39).<sup>[64]</sup> Thus, salicylaldehydes initially reacted with ethyl (triphenylphosphoranylidene)acetate in the presence of K<sub>2</sub>CO<sub>3</sub> under blue LED irradiation without requiring a photocatalyst. Once the





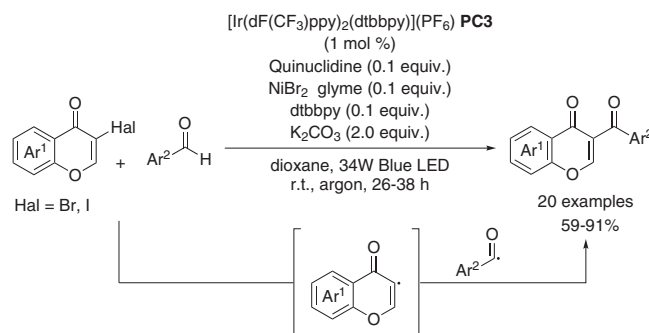
**Scheme 40.** Photoinduced Knoevenagel condensation for the synthesis of 2-imino-2H-chromene-3-carbonitriles.

Wittig/cyclic condensation reaction was completed, alkyl *N*-hydroxyphthalimide (NHPI) esters, *fac*-Ir(ppy)<sub>3</sub> (**PC1**) as photocatalyst, and DABCO as base were added directly to the reaction mixture, followed by further blue LED irradiation. Under these conditions, 3-alkylated coumarins were delivered from moderate yields with good functional group tolerance (22 examples, 32–74%).

A photocatalyzed condensation with salicylaldehydes is also involved in the synthesis of chromenes implemented by Singh and co-workers.<sup>[65]</sup> This process is initiated by the photoinduced activation of malononitrile, which undergoes a Knoevenagel condensation with a range of salicylaldehydes (Scheme 40). The subsequent intramolecular cyclization of the resulting Knoevenagel adduct provided substituted 2-imino-2H-chromene-3-carbonitriles in excellent yields (7 examples, 88–98%).

### 3. Reactivity of Chromene Derivatives under Visible-Light

The photochemical reactivity of chromene derivatives exemplifies the substantial potential of light-induced methodologies for accessing structurally diverse and complex heterocycles. These *O*-heterocyclic compounds are characterized by a highly conjugated  $\pi$ -system that promotes efficient light absorption, enabling a wide range of photochemical processes,<sup>[66]</sup> including radical formation, cyclization, and site-selective C–H functionalization. Recent advances in visible-light photoredox catalysis have significantly redefined the synthetic utility of these chromene-based analogs and related scaffolds, offering mild and efficacious procedures for synthesizing highly functionalized molecules that often avoid pre-functionalized starting materials while addressing the limitations or harsh conditions typically associated with conventional thermal methods.<sup>[5,6]</sup> Visible-light-promoted transformations such as Giese-type additions, decarboxylative cross-couplings, and oxidative cyclization reactions have proven particularly effective in functionalizing chromene derivatives, further demonstrating metal-free feasibility and emerging as environmentally friendly and sustainable alternatives to transition metal-catalyzed strategies,<sup>[67,68]</sup> significantly minimizing both costs and toxicity. The versatility of these reactions arises from the ability of chromene-based frameworks to



**Scheme 41.** Photoredox functionalization of 3-halogen/formyl chromones.

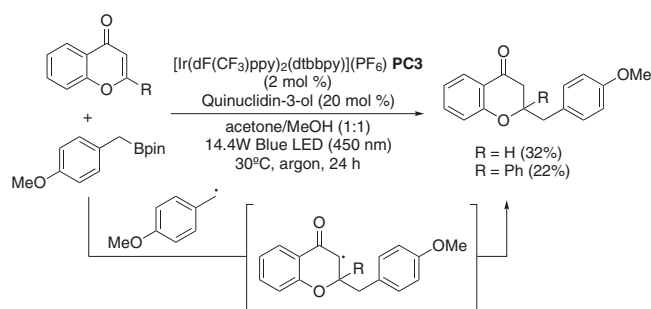
appropriately interact with excited-state photocatalysts, leading to efficient energy transfer ( $\pi \rightarrow \pi^*$ ) and facilitating radical stabilization. Thus, the unique electronic and structural features of chromene derivatives, including their inherent rigid planarity, are crucial in defining their specific reactivity profiles in visible light-mediated reactions. This underscores their flexibility as valuable synthons and emphasizes the benefits and wide-ranging applications of light-driven synthetic approaches in contemporary chemistry.

#### 3.1. Reactivity of Chromenones

##### 3.1.1. Reactivity of 4H-Chromenones (Chromones)

3-Substituted chromones are a relevant synthetic target with diverse applications.<sup>[23]</sup> As previously stated, one strategy for their preparation involves the consecutive cyclization–substitution of acyclic precursors. Alternatively, these compounds can be synthesized by the alkylation, acylation, or arylation of readily available 3-halochromone precursors.<sup>[69]</sup> In this context, Mkrtchyan and Iaroshenko described the transformation of 3-halochromones in 3-acyl-substituted chromones by means of dual visible-light photoredox/nickel catalysis (Scheme 41).<sup>[70]</sup> Reaction of 3-iodochromones with arylaldehydes using Ir/Ni catalytic system, K<sub>2</sub>CO<sub>3</sub> as base under blue LED irradiation, afforded the corresponding 3-acylchromones from moderate to high yields (16 examples, 59–91%). 3-Bromochromones were also suitable coupling partners and delivered the desired 3-acylchromone products (4 examples), with yields ranging between 67–71%. In further scope studies, they also demonstrated an alternative practical approach by reacting 3-formylchromones with arylbromides to achieve the same products with comparable yields (21 examples, 57–93%).

Among the radical reactions, the Giese reaction is probably the most widespread used in organic synthesis. Discovered 40 years ago, this process involves the conversion of a radical precursor to a nucleophilic radical intermediate, which is then trapped by an electron-deficient alkene to form a carbon–carbon bond.<sup>[71]</sup> Despite its utility, the classical Giese reaction is often hampered by a limited substrate scope, undesired side reactions, and the use of toxic reagents and solvents. However, recent advancements in photoredox catalysis have



**Scheme 42.** Photocatalyzed Giese-type addition of boronic esters to chromones.

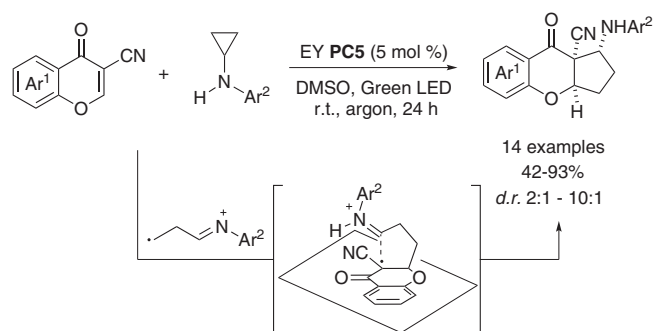
significantly enhanced this transformation by enabling the generation of carbon-centered radicals under mild and sustainable conditions, thereby improving the efficiency and applicability of existing methodologies on the Giese-type reactions.

Over the past few years, researchers described the generation of carbon-centered radicals from a wide range of precursors and explored their use in addition reactions with various electron-deficient alkenes, including chromenes, highlighting their synthetic versatility.<sup>[72]</sup>

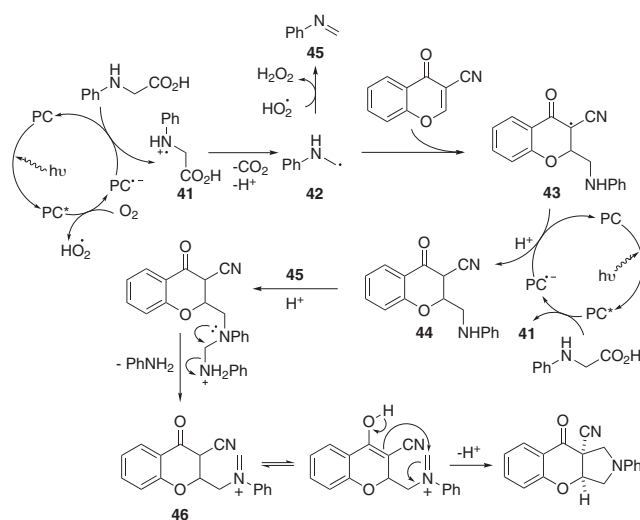
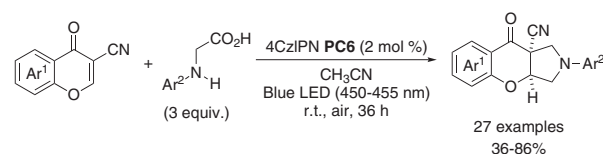
Lima et al. introduced a dual catalytic system formed by a photoredox catalyst and a Lewis base to generate carbon radicals from either boronic acids or esters, which subsequently reacted with electron-deficient olefins via radical addition to form the coupled products in a redox-neutral fashion.<sup>[73]</sup> Thus, the reaction of *p*-methoxybenzyl boronic ester and chromone in the presence of quinuclidin-3-ol as additive and an iridium complex **PC3** as photocatalyst, under blue LED irradiation, afforded the coupled chromane products in poor yields (Scheme 42).

Fused chromenes, incorporating both carbocyclic and heterocyclic rings, are key structural motifs found in several bioactive natural products.<sup>[74,75]</sup> Photocatalyzed cycloaddition has emerged as a powerful strategy for the synthesis of functionalized five-membered carbocycles and heterocycles.<sup>[76–78]</sup> In this context, photocycloaddition of chromone derivatives has recently attracted some attention as a valuable tool for the preparation of cyclopentanochromenes.

For instance, Albrecht and co-workers described the metal-free preparation of cyclopenta[*b*]chromenecarbonitrile derivatives via visible-light-promoted [3+2] cycloaddition reaction between substituted 3-cyanochromones and *N*-arylcyclopropylamines (Scheme 43).<sup>[79]</sup> The reaction was performed in the presence of organophotocatalyst Eosin Y (**PC5**) under irradiation with green light, resulting in the formation of the target cyclopenta[*b*]chromenecarbonitrile derivatives from moderate to excellent yields (14 examples, 42–93%) and good diastereoselectivities, ranging from 2:1 to 10:1. The diastereoselectivity of the process arises from steric factors during the approach of the radical intermediate to the substrate. In contrast, the electronic nature of the substituents on the starting materials had minimal impact, as the diastereomeric ratio remained relatively consistent across various substrates. Interestingly, introducing a strongly electron-withdrawing trifluoromethyl group on the *N*-cyclopropylaniline



**Scheme 43.** Organophotocatalyzed [3+2]-cycloaddition for the synthesis of cyclopenta[*b*]chromenecarbonitrile derivatives.



**Scheme 44.** Organophotocatalyzed [2+2+1] annulation of chromones with *N*-aryl glycines and proposed mechanism. “Reprinted (adapted) with permission from American Chemical Society. Copyright [2025].”

significantly enhanced diastereoselectivity, achieving the highest observed diastereoisomeric ratio. This suggests that while steric effects dominate, certain substituents may also influence the diastereomeric outcome by stabilizing the transition state.

Another example of a metal-free photocatalyzed cycloaddition involving 3-cyanochromones as starting materials for the preparation of fused chromenes was described by Zhou et al. in 2023.<sup>[80]</sup> In this study, an organophotocatalyzed aerobic decarboxylative [2+2+1] annulation of chromones with *N*-aryl glycines was developed for the synthesis of chromenopyrrolidines (27 examples, 36–86%, Scheme 44). The reaction of 3-cyanochromones and *N*-aryl glycines was conducted in the presence of 1,2,3,5-tetrakis(carbazol-9-yl)-4,6-dicyanobenzene (4CzIPN, **PC6**) as the photocatalyst under irradiation of blue light. Mechanistic studies suggest that, under visible-light irradiation, the photocatalyst 4CzIPN is excited ( $PC^*$ ) and then

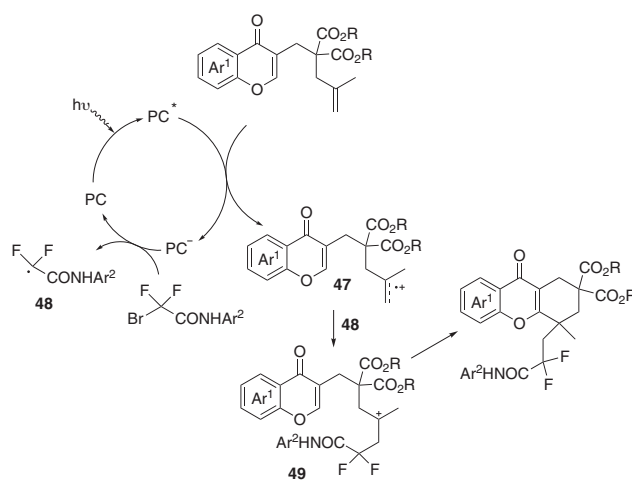
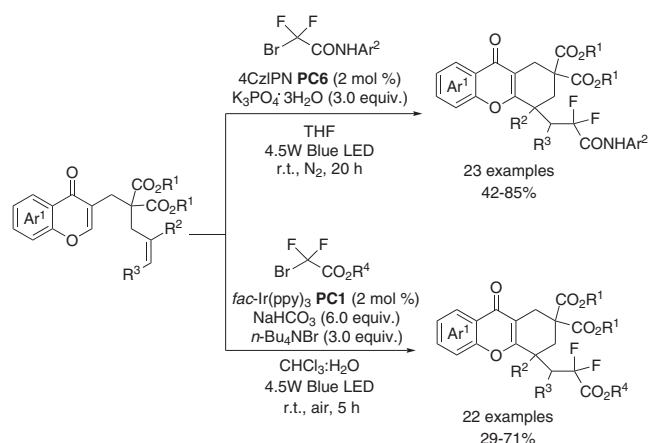
reductively quenched by *N*-phenylglycine to form radical cation **41**. Subsequent deprotonation and decarboxylation yield the aminomethyl radical **42**, which undergoes Giese-type addition to the cyanochromone, generating radical **43**. A single-electron reduction of **43** by  $\text{PC}^{\bullet-}$ , followed by protonation, produces intermediate **44**. Alternatively, the catalytic cycle can proceed through single-electron transfer (SET) between molecular oxygen and  $\text{PC}^{\bullet-}$ , generating a hydroperoxyl radical, which can oxidize **42** to imine **45**. Next, a nucleophilic addition of amine **44** to imine **45**, followed by elimination of aniline generates iminium **46**, which triggers the intramolecular Mannich reaction, allowing the pyrrolidine ring formation (Scheme 44).

The authors suggest that the steric and electronic properties of the substrates guide the selective formation of one iminium intermediate over others, which in turn dictates the outcome of the cyclization. The reaction requires two equivalents of *N*-arylglycine in which one is used for radical initiation and the other for imine formation. To minimize the potential oxidative dimerization of *N*-arylglycines, the first stage of the reaction (Giese-type addition) was carried out under an inert atmosphere, while the subsequent cyclization step was performed under open-air conditions.

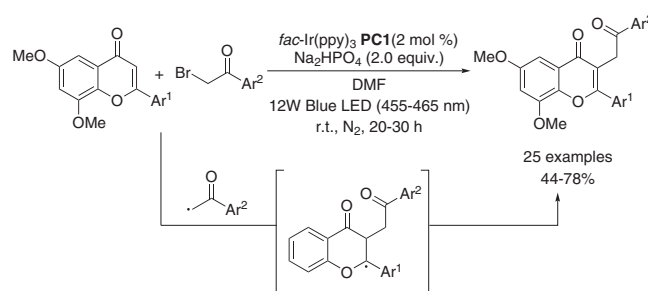
In a more recent contribution to visible light-mediated annulation of chromones, Wang et al. reported the reaction of 3-substituted chromone derivatives with either bromodifluoroacetamides or bromodifluoroacetates as coupling partners affording a broad range of fused chromone analogs.<sup>[81]</sup> Thus, reaction of 2-(2-methylallyl)-2-[(4-oxo-4*H*-chromen-3-yl)methyl]malonate and 2-bromo-2,2-difluoro-*N*-phenylacetamide in the presence of 4CzIPN (**PC6**) as photocatalyst and  $\text{K}_3\text{PO}_4 \cdot 3\text{H}_2\text{O}$  as base under blue LED irradiation gave desired fused chromone products from moderate to good yields (23 examples, 42–85%, Scheme 45). Bromodifluoroacetate ester was also used as an efficient radical difluoroacetate precursor; however, the optimized reaction conditions were slightly different, requiring the use of *fac*-Ir(ppy)<sub>3</sub> (**PC1**) as photocatalyst and  $\text{NaHCO}_3$  as base. Under these conditions, the target products (22 examples) were isolated, with yields ranging between 29–71%.

A possible reaction pathway begins with the excitation of the photocatalyst 4CzIPN\*, which oxidizes the C=C double bond of the chromone derivative, yielding the radical cation intermediate **47** along with 4CzIPN<sup>•−</sup>. The latter is then oxidized by bromodifluoroacetamide, generating the difluoroacetamide radical intermediate **48** and restoring ground-state 4CzIPN, ready for the next catalytic cycle. Next, the coupling of intermediate **48** with the radical cation intermediate **47** forms a carbocationic intermediate **49**, which on intramolecular cyclization and further deprotonation give the desired product.

Biflavonoids are dimers of flavonoid (2-arylchromone) structures that have been isolated from various plants and are known for their diverse biological activities. Despite their pharmacological potential, the chemistry and biology of these compounds remain underexplored, likely due to the absence of efficient synthetic methods. Some relevant examples include radical-based approaches, such as the CAN-mediated radical coupling of appropriately substituted diaryl-1,3-diketones described by

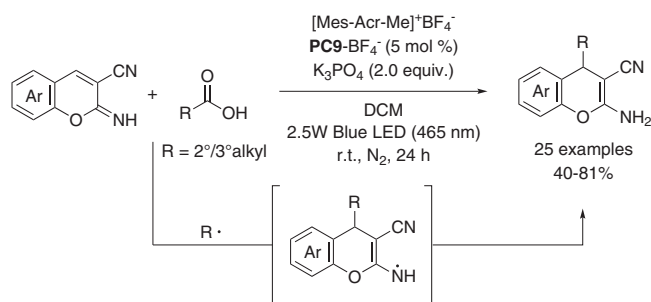


**Scheme 45.** Visible-light-triggered difluoroacetylation/cyclization of chromone-tethered alkenes and proposed mechanism. "Reprinted (adapted) with permission from American Chemical Society. Copyright (2025)."

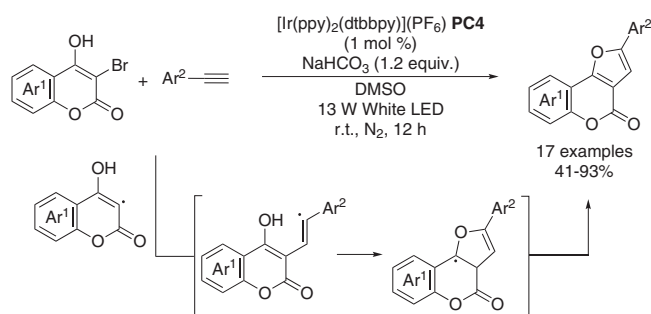


**Scheme 46.** Photocatalyzed radical alkylation of flavones.

Nanjan and Banjeri,<sup>[82]</sup> and the  $\text{SmI}_2$ -promoted temperature-controlled stereodivergent radical coupling of flavones reported by Soto et al.<sup>[83]</sup> However, both methodologies are restricted to the preparation of symmetric biflavonoids. Addressing this limitation, Fregoso-López and Miranda reported in 2022 the first synthesis of non-symmetrical biflavones, using as key step the visible-light iridium-catalyzed radical C3 alkylation of flavones with phenacyl bromides (25 examples, 44–78%, Scheme 46).<sup>[84]</sup> The reaction proceeds via a single-electron transfer (SET) from the excited photocatalyst to generate a radical-anion, which undergoes C–Br cleavage to form an electrophilic  $\alpha$ -acyl radical.



**Scheme 47.** Metal-free visible-light-induced decarboxylative C4-alkylation of 2-iminochromenes.



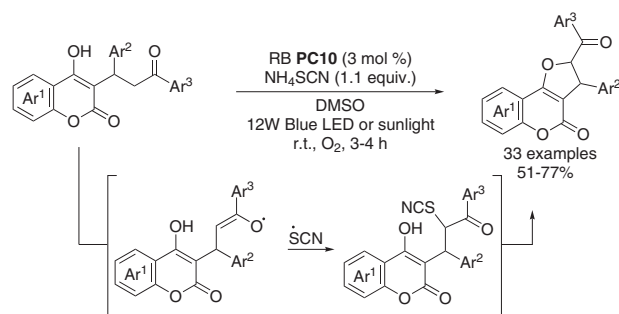
**Scheme 48.** Photocatalyzed radical alkyne insertion with 3-bromo-4-hydroxycoumarins.

This radical then undergoes a Giese-type addition at the C3 position of the flavone, followed by oxidation by the Ir(III) complex, which regenerates the photocatalyst. The resulting alkyl flavones were subsequently subjected to selective demethylation through a Baker–Venkataraman rearrangement in the presence of acyl chlorides to obtain 3,3'-biflavones (19 examples, 42–87%).

### 3.1.2. Reactivity of 2H-chromenones (coumarins)

Singh and co-workers developed a regioselective metal-free photocatalytic strategy for the decarboxylative C-4 alkylation of 2-imino-2H-chromene-carbonitriles.<sup>[85]</sup> Upon blue LED irradiation, the acridinium photocatalyst  $[\text{Mes-Acr-Me}]^+\text{BF}_4^-$  (PC9-BF<sub>4</sub><sup>−</sup>) efficiently generates alkyl radicals from aliphatic carboxylic acids, which selectively attack the 2-iminochromene moiety, delivering C-4 alkylated products from moderate to high yields (25 examples, 40–81%, Scheme 47). Both secondary and tertiary carboxylic acids are compatible, including sterically hindered ones. As expected, primary substrates failed to yield the corresponding alkylated product, likely due to the poor stability of primary alkyl radicals. The process was successfully scaled up to a gram-scale.

The first visible-light-mediated transformation of a coumarin derivative was reported by Zhou et al. in 2016.<sup>[86]</sup> They described an efficient synthesis of furo[3,2-c]coumarins through photocatalyzed alkyne insertion of 3-bromo-4-hydroxycoumarins. Reaction of alkynes and 3-bromo-4-hydroxycoumarins in the presence of  $[\text{Ir}(\text{ppy})_2(\text{dtbbpy})](\text{PF}_6)$  (PC4) as photocatalyst, under white LED irradiation, afforded a series of furocoumarin analogs from moderate to high yields (17 examples, 41–93%, Scheme 48).



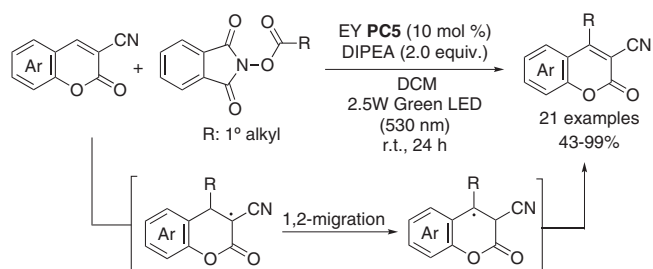
**Scheme 49.** Metal-free visible-light-induced cross-dehydrogenative oxygenation of Warfarin analogs.

Electron-rich and neutral phenylacetylenes gave the highest yields as their electronic properties facilitate efficient radical addition (93% for *p*-*tert*-butylphenylacetylene). In contrast, electron-deficient acetylenes performed poorly (22% for *p*-chlorophenylacetylene). The process is carried out without stoichiometric oxidants and operates under mild conditions in a redox-neutral fashion. A possible catalytic cycle involves the homolytic cleavage of the C–Br bond and subsequent addition of the resulting radical to the alkyne to generate an intermediate vinyl radical. The vinyl radical intermediate then attacks the carbonyl group intramolecularly to give radical intermediate, which on oxidation and deprotonation finally affords the furocoumarin.

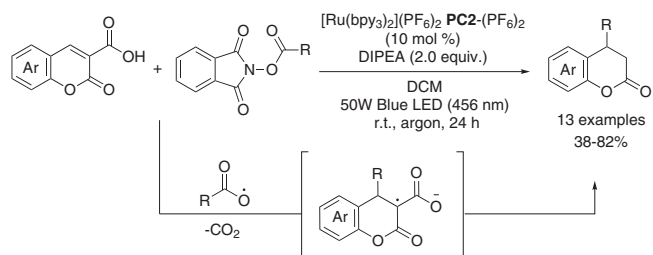
In a more recent study, Brahmachari and co-workers developed the metal-free photocatalyzed synthesis of structurally related dihydrofuro[3,2-c]chromen-2-ones from warfarin derivatives via intramolecular C–O bond formation through Csp<sup>3</sup>–H cross-dehydrogenative oxygenation.<sup>[87]</sup> The reaction is promoted by blue LED light or sunlight in the presence of non-toxic organic dye Rose Bengal (PC10) as photocatalyst, NH<sub>4</sub>SCN as additive, and molecular oxygen as the oxidant, enabling the formation of a wide range of warfarin analogs from moderate to good yields (33 examples, 51–77%, Scheme 49). The reaction proceeds by means of the formation of an enoxy radical, subsequent diradical coupling with thiocyanate radical and intramolecular nucleophilic substitution to finally provide dihydrofurocoumarins.

Another relevant example of metal-free photocatalyzed transformations of coumarin derivatives is the regioselective decarboxylative C4-alkylation using *N*-(acyloxy)phthalimides as radical precursors, reported by Singh and co-workers in 2020.<sup>[88]</sup> This methodology achieves moderate to quantitative yields (21 examples, 43–99%) of C4-alkylated coumarins in the presence of *N,N*-diisopropylethylamine (DIPEA) and Eosin Y (PC5) as photocatalyst under green LED irradiation (Scheme 50). The process is initiated by the formation of an alkyl radical via elimination of phthalimide and release of carbon dioxide. Subsequently, the addition of the alkyl radical to coumarin generated a radical intermediate in position C-3, which then migrates to position C-4. Finally, oxidation to the corresponding carbocation followed by deprotonation furnished desired alkylated coumarins. The process is restricted to primary alkyl groups; interestingly, when the reaction was performed with secondary or tertiary alkyl





**Scheme 50.** Metal-free visible-light-promoted decarboxylative C4-alkylation of coumarins using NHPI esters.



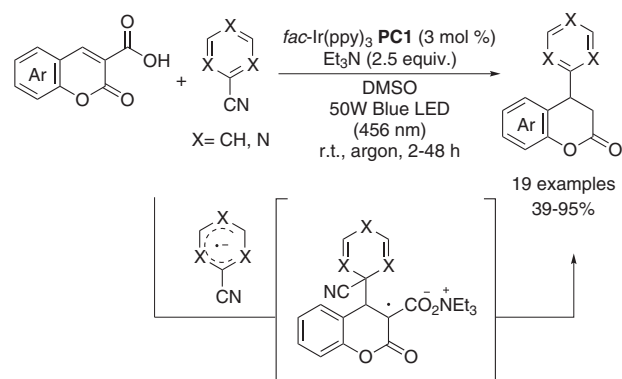
**Scheme 51.** Photocatalyzed Giese reaction of coumarin-4H-chromone-3-carboxylic acids using NHPI esters as radical precursors.

groups, the products from the Giese reaction were isolated from moderate to quantitative yields (10 examples, 50–86%).

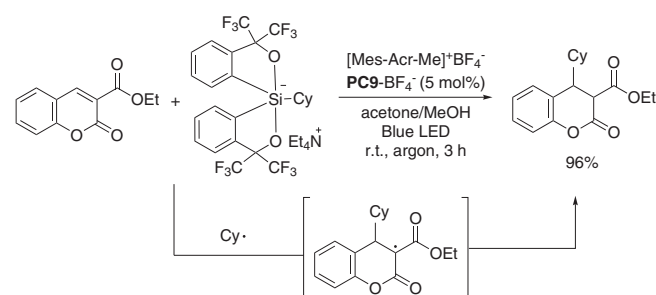
Giese-type transformations have been extensively used to functionalize coumarin derivatives at the C4-position.<sup>[71,72]</sup> For example, Albrecht and co-workers described in 2021 a photocatalyzed Giese reaction for the C4-functionalization of chromone-3-carboxylic acids.<sup>[89]</sup> Thus, reaction of coumarins with *N*-(acyloxy)phthalimides as radical precursors in the presence of DIPEA and Ru-based photoredox catalyst, under blue LED light, afforded 4-substituted-chroman-2-ones from moderate to good yields (13 examples, 38–82%, Scheme 51). The reaction succeeded when using secondary and tertiary alkyl radicals but failed with primary and benzylic radicals, probably due to lack of stability and competing radical dimerization.

Later, in 2022, the same authors expanded the reactivity of coumarin-3-carboxylic acids as Giese substrates, developing their decarboxylative reductive azaarylation reaction.<sup>[90]</sup> This methodology uses (cyano)azaarenes as radical precursors in the presence of NEt<sub>3</sub> and *fac*-Ir(ppy)<sub>3</sub> (PC1) as photocatalyst under blue LED irradiation, achieving moderate to high yields of the corresponding C4-functionalized products (19 examples, 39–95%, Scheme 52). This photocatalytic process is very relevant from the synthetic point of view, enabling the efficient synthesis of pharmaceutically relevant pyridine–coumarin hybrids.<sup>[91,92]</sup>

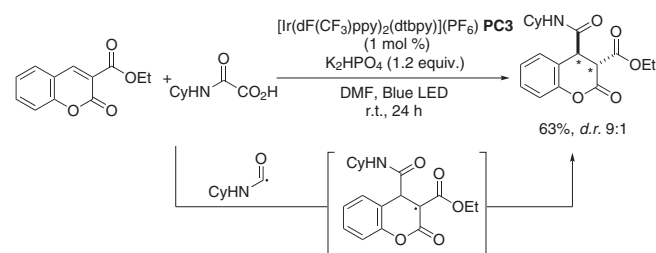
Morofuji et al. reported an innovative photocatalytic Giese-type reaction of coumarin-3-carboxylates using a novel class of alkylsilicates bearing C,O-bidentate ligands as radical precursors.<sup>[93]</sup> The reaction proceeds in the presence of organic acridinium-based photocatalyst [Mes-Acr-Me]<sup>+</sup>BF<sub>4</sub><sup>−</sup> (PC9-BF<sub>4</sub><sup>−</sup>) under blue LED irradiation, giving the corresponding C4-cyclohexyl adduct in a nearly quantitative manner (Scheme 53).



**Scheme 52.** Photocatalyzed decarboxylative Giese azaarylation of coumarin-3-carboxylic acids.



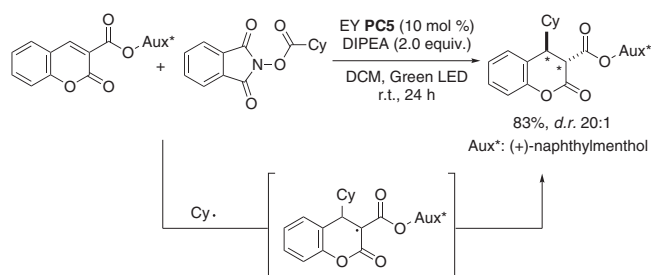
**Scheme 53.** Organophotocatalyzed Giese-type alkylation of ethyl coumarin-3-carboxylate.



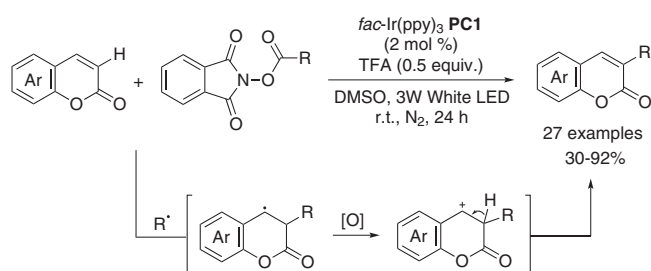
**Scheme 54.** Stereoselective photoinduced Giese amidation of ethyl coumarin-3-carboxylate.

In a Giese amidation reported in 2023, Lee and co-workers introduced bench-stable, non-toxic oxamic acids as carbamoyl radical precursors.<sup>[94]</sup> The methodology can be applied to a broad scope of Michael acceptors, accommodating both exocyclic and *endo*-cyclic systems, including coumarin-derived substrates. Thus, the reaction of ethyl coumarin-3-carboxylate and *N*-cyclohexyl oxamic acid as the radical source in the presence of an Ir-based photoredox catalyst PC3 under irradiation with blue LED light afforded the desired 4-carbamoylcoumarin in a 63% yield with good *trans*-diastereoselectivity (*d.r.* 9:1) (Scheme 54).

Singh and his team recently developed a diastereoselective Giese addition on activated coumarin-3-carboxylates featuring chiral auxiliaries, marking notable progress in stereoselective functionalization of coumarin derivatives.<sup>[95]</sup> Reaction of coumarins and *N*-hydroxyphthalimide esters in the presence of organophotocatalyst Eosin Y (PC5) under green LED irradiation, delivered a series of chiral coumarin derivatives in good yields



**Scheme 55.** Stereoselective metal-free visible-light-promoted Giese addition to coumarins.

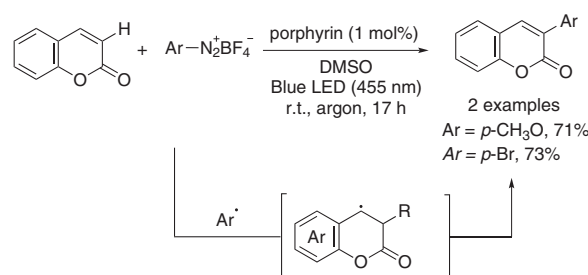


**Scheme 56.** Photocatalyzed C3-alkylation of coumarin via oxidative coupling reaction with alkyl NHPH esters.

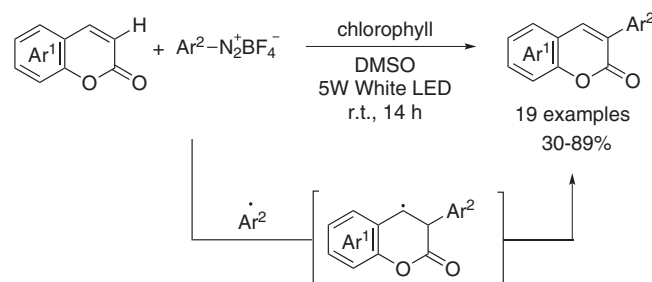
(16 examples, 76–94%) and remarkable diastereoselectivity (up to d.r. 20:1, Scheme 55). The carboxylate group at the C-3 position served as both an anchoring point for the auxiliary and a polarizing group to enhance C-4 electrophilicity, thereby facilitating the radical attack.

In coumarin chemistry, much of the attention has been focused on regioselective transformations at the C-4 position, the most active site for Giese-type mechanisms, as illustrated above. However, the C-3 position stands out as the most nucleophilic site, highly susceptible to electrophilic metalation and direct C–H activation. Leveraging this reactivity and recognizing the ubiquitous presence of the 3-substituted coumarin scaffold in biologically active compounds,<sup>[96,97]</sup> Jin et al. described the first example of the direct regioselective C3-alkylation of coumarins through a decarboxylative coupling process.<sup>[98]</sup> Reaction of coumarins and *N*-hydroxyphthalimide esters as alkylating agents in the presence of TFA as additive and *fac*-Ir(ppy)<sub>3</sub> (PC1) as photocatalyst, under blue LED irradiation, produced 3-alkylated coumarins from moderate to excellent yields (27 examples, 30–92%, Scheme 56). The proposed mechanism for this transformation involves the formation of an alkyl radical from phthalimide and subsequent addition to coumarin. The generated radical intermediate is further oxidized to a carbocation, which deprotonates to finally afford the alkylated coumarin.

A greener contribution to the functionalization of the C3-position was made by Gryko and co-workers, reporting their pioneering study on the use of porphyrins and diazonium salts for the direct metal-free C–H arylation of various heteroarenes and coumarins in good yields, under blue LED irradiation (Scheme 57).<sup>[99]</sup> Remarkably, the efficiency of the porphyrin organocatalyst in facilitating oxidative quenching depends on



**Scheme 57.** Metal-free visible-light-promoted C3-arylation of coumarin with diazonium salts, using porphyrins.



**Scheme 58.** Metal-free visible-light-promoted C3-arylation of coumarin with diazonium salts, using natural pigment chlorophyll as the photosensitizer.

its redox properties, which were fine-tuned by peripheral substituents.

Moazzam and Jafarpour subsequently described another intriguing example of metal-free photocatalyzed C3-activation of coumarins.<sup>[100]</sup> The authors performed a visible-light-induced metal-free C3-arylation of coumarins, employing aryl diazonium salts as arylating agents and chlorophyll as natural photocatalyst under white LED irradiation (Scheme 58). This sustainable approach takes advantage of a renewable biocatalyst and mild reaction conditions to efficiently prepare 3-aryl coumarins, with excellent regioselectivity, from moderate to high yields (19 examples, 30–89%) and scalability up to gram-scale synthesis, highlighting the potential of natural photocatalysts in modern green chemistry.

## 4. Summary and Outlook

Chromene derivatives are a versatile class of heterocyclic compounds with considerable significance in organic synthesis, biological research, and medicinal chemistry. This review has highlighted the transformative potential of visible-light-mediated approaches in chromene chemistry, offering greener and more efficient pathways for their synthesis and functionalization. The application of photochemical strategies has notably improved atom economy and synthetic efficiency while often eliminating the need for transition metals, thereby aligning with the principles of green chemistry. Furthermore, these advancements have facilitated access to previously challenging chromene derivatives, broadening the chemical space available for modern drug discovery. Several key innovative methodologies, including Giese-type transformations,

multicomponent reactions (MCRs), and cascade processes, have been instrumental in achieving this progress in visible-light-driven procedures. Giese-type additions, characterized by radical addition to electron-deficient alkenes, provide versatile and effective means for chromene functionalization. Similarly, MCRs enable the construction of complex chromene frameworks in a single step, maximizing efficiency and reducing waste. Beyond these, photocatalytic strategies have enabled a variety of other transformations, including oxidative cyclizations, cross-dehydrogenative couplings, and radical-triggered cascade reactions, each contributing to the structural and functional diversity of chromene derivatives. Particularly, the potential for catalyst-free, metal-free, and even solvent-free reactions has emerged as a frontier in chromene synthesis. Such approaches not only simplify reaction conditions but also reduce environmental impact, further enhancing the sustainability of these methods. These developments reflect the ongoing efforts to refine synthetic methodologies while addressing green and economic concerns. Nevertheless, despite significant progress, challenges persist as the stereoselective synthesis of chromene frameworks using visible-light-driven processes remains underexplored. Considering the critical importance of chiral molecules in pharmaceutical applications, developing stereoselective photocatalytic strategies could unlock new opportunities in drug discovery.

In conclusion, the integration of photocatalysis, green chemistry principles, and innovative reaction mechanisms has boosted chromene chemistry into a new era. The ability to conduct complex transformations under mild and sustainable conditions underscores the growing potential of this field. Ongoing efforts to overcome current limitations and expand the scope of these methodologies will ensure that chromene-derived scaffolds remain at the forefront of organic synthesis, medicinal chemistry, and materials science in future research.

## Acknowledgments

This work has received financial support from Eidikos Logarias-mos Kondilion kai Ereunas, University of Patras (ELKE PATRAS) under the call MEDICUS as well as from the Instituto de Salud Carlos III (PI22/00148) and MCI (PID2022-137893OB-I00). P. P. R. thanks Programa Investigo for a predoctoral contract (AYUD/2022/9313, EU Next Generation). The authors sincerely thank the ACS and RSC for granting permission to use and adapt figures and schemes from their publications under the Creative Commons Attribution-NonCommercial 3.0 Unported Licence.

## Conflict of Interests

The authors declare no conflict of interest.

## Data Availability Statement

Data sharing is not applicable to this article as no new data were created or analyzed in this study.

**Keywords:** chromenes · chromenones · green chemistry · photocatalysis · visible-light

- [1] a) A. T. Benny, S. D. Arikatt, C. G. Vazhappilly, S. Kannadasan, R. Thomas, M. S. N. Leelabaiamma, E. K. Radhakrishnan, P. Shanmugam, *Mini Rev. Med. Chem.* **2022**, *22*, 1030; b) V. Raj, J. Lee, *Front. Chem.* **2020**, *8*, 623; c) C. F. M. Silva, V. F. Batista, D. C. G. A. Pinto, A. M. S. Silva, *Expert Opin. Drug Discovery* **2018**, *13*, 795; d) J. Reis, A. Gaspar, N. Milhazes, F. Borges, *J. Med. Chem.* **2017**, *60*, 7941.
- [2] a) A. Singh, K. Singh, K. Kaur, A. Singh, A. Sharma, K. Kaur, J. Kaur, G. Kaur, U. Kaur, H. Kaur, P. Singh, P. M. S. Bedi, *Biomedicines* **2024**, *12*, 1192; b) U. Agarwal, S. Verma, R. K. Tonk, *Bioorg. Med. Chem. Lett.* **2024**, *111*, 129912; c) V. M. Patil, N. Masand, S. Verma, V. Masand, *Chem. Biol. Drug Des.* **2021**, *98*, 943; d) F. Annunziata, C. Pinna, S. Dallavalle, L. Tamborini, A. Pinto, *Int. J. Mol. Sci.* **2020**, *21*, 4618; e) F. Esposito, F. A. Ambrosio, R. Maleddu, G. Costa, R. Rocca, E. Maccioni, R. Catalano, I. Romeo, P. Eleftheriou, D. C. Karia, P. Tsirides, N. Godvani, H. Pandya, A. Corona, S. Alcaro, A. Artese, A. Geronikaki, E. Tramontano, *Eur. J. Med. Chem.* **2019**, *182*, 111617; f) C. F. M. Silva, D. C. G. A. Pinto, A. M. S. Silva, *ChemMedChem* **2016**, *11*, 2252; g) S. Emami, S. Dadashpour, *Eur. J. Med. Chem.* **2015**, *102*, 611.
- [3] a) X.-M. Cai, Y. Lin, J. Zhang, Y. Li, Z. Tang, X. Zhang, Y. Jia, W. Wang, S. Huang, P. Alam, Z. Zhao, B. Z. Tang, *Natl. Sci. Rev.* **2023**, *10*, nwad233; b) K. Ma, L. Zhao, Y. Yue, C. Yin, *Chem. Phys. Rev.* **2022**, *3*, 011302; c) F. A. Mohamed, M. B. Sheier, M. M. Reda, H. M. Ibrahim, *Curr. Org. Synth.* **2022**, *19*, 757; d) D. Cao, Z. Liu, P. Verwilt, S. Koo, P. Jangjili, J. S. Kim, W. Lin, *Chem. Rev.* **2019**, *119*, 10403; e) M. Costa, T. A. Dias, A. Brito, F. Proença, *Eur. J. Med. Chem.* **2016**, *123*, 487.
- [4] a) N. V. Vchislo, E. A. Verochkina, *Eur. J. Org. Chem.* **2024**, *27*, e202400552; b) S.-L. Zhenga, L. Chen, *Org. Biomol. Chem.* **2021**, *19*, 10530; c) M. K. Katiyar, G. K. Dhakad, Shivani, S. A., S. Bhagat, T. Arora, R. Kumar, *J. Mol. Struct.* **2022**, *1263*, 133012; d) M. Mamaghani, R. H. Nia, F. Tavakoli, P. Jahanshahi, *Curr. Org. Chem.* **2018**, *22*, 1704; e) R. Pratap, V. J. Ram, *Chem. Rev.* **2014**, *114*, 10476.
- [5] a) L. Marzo, S. K. Pagire, O. Reiser, B. Kçnig, *Angew. Chem., Int. Ed.* **2018**, *57*, 10034; b) M. H. Shaw, J. Twilton, D. W. C. MacMillan, *J. Org. Chem.* **2016**, *81*, 6898; c) J. M. R. Narayanam, C. R. J. Stephenson, *Chem. Soc. Rev.* **2011**, *40*, 102.
- [6] a) F. Mohamadpour, A. M. Amani, *RSC Adv.* **2024**, *14*, 20609; b) J. D. Bell, J. A. Murphy, *Chem. Soc. Rev.* **2021**, *50*, 9540; c) L. Guillemard, J. Wencel-Delord, *Beilstein J. Org. Chem.* **2020**, *16*, 1754; d) C.-S. Wang, P. H. Dixneuf, J.-F. Soule, *Chem. Rev.* **2018**, *118*, 7532; e) J. Xie, H. Jin, A. S. K. Hashmi, *Chem. Soc. Rev.* **2017**, *46*, 5193; f) N. A. Romero, D. A. Nicewicz, *Chem. Rev.* **2016**, *116*, 10075; g) C. K. Prier, D. A. Rankin, D. W. C. MacMillan, *Chem. Rev.* **2013**, *113*, 5322.
- [7] Y. Zhao, Y. Lv, W. Xia, *Chem. Rev.* **2019**, *19*, 424.
- [8] a) G. E. M. Crisenza, P. Melchiorre, *Nat. Commun.* **2020**, *11*, 803; b) T. Yoon, M. Ischay, J. Du, *Nat. Chem.* **2010**, *2*, 527.
- [9] a) V. Patel, T. Bambharoliya, D. Shah, D. Patel, M. Patel, U. Shah, M. Patel, S. Patel, N. Solanki, A. Mahavar, A. Nagani, H. Patel, M. Rathod, B. Bhimani, V. Bhavsar, S. Padhiyar, S. Koradia, C. Chandarana, B. Patel, R. C. Dabhi, A. Patel, *Curr. Top. Med. Chem.* **2024**, *25*, 437. <https://doi.org/10.2174/0115680266305231240712104736>; b) A. Ghatak, A. Pramanik, M. Das, *Tetrahedron* **2022**, *106*, 132628.
- [10] a) R. L. Mohlala, T. J. Rashamuse, E. M. Coyanis, *Front. Chem.* **2024**, *12*, 1469677; b) B. A. D. Neto, R. O. Rocha, M. O. Rodrigues, *Molecules* **2022**, *27*, 132; c) S. E. John, S. Gulatia, N. Shankaraiah, *Org. Chem. Front.* **2021**, *8*, 4237; d) R. C. Cioc, E. Ruijter, R. V. A. Orru, *Green Chem.* **2014**, *16*, 2958; e) A. Dömling, *Chem. Rev.* **2006**, *106*, 17.
- [11] a) S. Ariya, M. Neetha, G. Anilkumar, *Curr. Catal.* **2023**, *12*, 17. b) G. A. Coppola, S. Pillitteri, E. V. Van der Eycken, S.-L. You, U. K. Sharma, *Chem. Soc. Rev.* **2022**, *51*, 2313; c) S. Garbarino, D. Ravelli, S. Protti, A. Basso, *Angew. Chem., Int. Ed.* **2016**, *55*, 15476.
- [12] D. Jaiswal, A. Mishra, P. Rai, M. Srivastava, B. P. Tripathi, S. Yadav, J. Singh, J. Singh, *Res. Chem. Intermed.* **2018**, *44*, 231.
- [13] A. K. Sharma, J. Tiwari, D. Jaiswal, S. Singh, J. Singh, J. Singh, *Curr. Organocatal.* **2019**, *6*, 222.
- [14] Z. Jalili, R. Tayebbe, F. M. Zonoz, *RSC Adv.* **2021**, *11*, 18026.
- [15] M. Jarrahi, R. Tayebbe, B. Maleki, A. Salimi, *RCS Adv.* **2021**, *11*, 19723.

- [16] L. Chen, C. Lin, Y. Lan, Z. Li, D. Huang, W. Yang, Y. Li, *Environ. Chem. Lett.* **2020**, *18*, 2157.
- [17] S. Karreman, S. B. H. Karnbrock, S. Kolle, C. Golz, M. Alcarazo, *Org. Lett.* **2021**, *23*, 1991.
- [18] M. D. Heredia, M. Puiatti, R. A. Rossi, M. E. Budén, *Org. Biomol. Chem.* **2022**, *20*, 228.
- [19] N. Tanaka, S. R. Mitton-Fry, M. U. Hwang, J. L. Zhu, K. A. Scheidt, *ACS Catal.* **2024**, *14*, 7949.
- [20] S. K. Sharma, S. Kumar, K. Chand, A. Kathuria, A. Gupta, R. Jain, *Curr. Med. Chem.* **2011**, *18*, 3825.
- [21] a) A. Gaspar, E. M. P. J. Garrido, F. Borges, J. M. P. J. Garrido, *ACS Omega* **2024**, *9*, 21706; b) C. M. M. Santos, A. M. S. Silva, *Adv. Heterocycl. Chem.* **2022**, *138*, 159; c) R. S. Keri, S. Budagumpi, R. K. Pai, R. G. Balakrishna, *Eur. J. Med. Chem.* **2014**, *78*, 340; d) A. Gaspar, M. J. Matos, J. Garrido, E. Uriarte, F. Borges, *Chem. Rev.* **2014**, *114*, 4960.
- [22] a) P. S. Auti, S. Jagetiya, A. T. Paul, *Chem. Biodiversity* **2023**, *20*, e202300587; b) S. Tian, T. Luo, Y. Zhu, J.-P. Wan, *Chin. Chem. Lett.* **2020**, *31*, 3073; c) V. F. Vavsari, S. Balalaie, *Chem. Heterocycl. Comp.* **2020**, *56*, 404; d) N. A. Mohsin, M. Irfan, S. Hassan, U. Saleem, *Pharm. Chem. J.* **2020**, *54*, 241; e) R. Kshatriya, V. P. Jejurkar, S. Saha, *Tetrahedron* **2018**, *74*, 811; f) S. Emami, Z. Ghanbarimasir, *Eur. J. Med. Chem.* **2015**, *93*, 539.
- [23] a) V. Y. Sosnovskikh, *Chem. Heterocycl. Comp.* **2020**, *56*, 1111; b) A. T. Gordon, I. D. I. Ramaite, S. S. Mnyakeni-Moleele, *Arkivoc* **2020**, *2020*, 148; c) V. A. Litvinova, A. S. Tikhomirov, *Chem. Heterocycl. Comp.* **2018**, *54*, 923; d) M. Y. Kornev, V. Y. Sosnovskikh, *Chem. Heterocycl. Comp.* **2016**, *52*, 71; e) A. Gaspar, J. Reis, A. Fonseca, N. Milhazes, D. Viña, E. Uriarte, F. Borges, *Bioorg. Med. Chem. Lett.* **2011**, *21*, 707.
- [24] a) T. Guo, L. Bi, M. Zhang, C.-J. Zhu, L.-B. Yuan, Y.-H. Zhao, *J. Org. Chem.* **2022**, *87*, 16907; b) T. Luo, H. Wu, L.-H. Liao, J.-P. Wan, Y. Liu, *J. Org. Chem.* **2021**, *86*, 15785; c) T. Luo, J.-P. Wan, Y. Liu, *Org. Chem. Front.* **2020**, *7*, 1107; d) P. N. Bagle, M. V. Mane, S. P. Sancheti, A. B. Gade, S. R. Shaikh, M. H. Baik, N. T. Patil, *Org. Lett.* **2019**, *21*, 335; e) L. Fu, J. Wan, *Asian J. Org. Chem.* **2019**, *8*, 767; f) Y. Guo, Y. Xiang, L. Wei, J.-P. Wan, *Org. Lett.* **2018**, *20*, 3971.
- [25] H. Xiang, Q. Zhao, Z. Tang, J. Xiao, P. Xia, C. Wang, C. Yang, X. Chen, H. Yang, *Org. Lett.* **2017**, *19*, 146.
- [26] a) T. Chatterjee, N. Iqbal, Y. You, E. J. Cho, *Acc. Chem. Res.* **2016**, *49*, 2284; b) H.-R. Zhang, D.-Q. Chen, Y.-P. Han, Y.-F. Qiu, D.-P. Jin, X.-Y. Liu, *Chem. Commun.* **2016**, *52*, 11827; c) L. Zhu, L.-S. Wang, B. Li, B. Fu, C.-P. Zhang, W. Li, *Chem. Commun.* **2016**, *52*, 6371; d) W. Yu, X.-H. Xu, F.-L. Qing, *Org. Lett.* **2016**, *18*, 5130; e) M. Zhang, W. Li, Y. Duan, P. Xu, S. Zhang, C. Zhu, *Org. Lett.* **2016**, *18*, 3266; f) Q.-Y. Lin, Y. Ran, X.-H. Xu, F.-L. Qing, *Org. Lett.* **2016**, *18*, 2419; g) L. Li, X. Mu, W. Liu, Y. Wang, Z. Mi, C.-J. Li, *J. Am. Chem. Soc.* **2016**, *138*, 5809; h) W. Fu, X. Han, M. Zhu, C. Xu, Z. Wang, B. Ji, X.-Q. Hao, M.-P. Song, *Chem. Commun.* **2016**, *52*, 13413; i) J. Rong, L. Deng, P. Tan, C. Ni, Y. Gu, J. Hu, *Angew. Chem., Int. Ed.* **2016**, *55*, 2743; j) T. Koike, M. Akita, *Acc. Chem. Res.* **2016**, *49*, 1937; k) J. J. Douglas, H. Albright, M. J. Sevrin, K. P. Cole, C. R. J. Stephenson, *Angew. Chem., Int. Ed.* **2015**, *54*, 14898; l) S. Barata-Vallejo, S. M. Bonesi, A. Postigo, *Org. Biomol. Chem.* **2015**, *13*, 11153; m) C. Yu, N. Iqbal, S. Park, E. J. Cho, *Chem. Commun.* **2014**, *50*, 12884; n) J. Xie, X. Yuan, A. Abdulkader, C. Zhu, J. Ma, *Org. Lett.* **2014**, *16*, 1768; o) P. Xu, J. Xie, Q. Xue, C. Pan, Y. Cheng, C. Zhu, *Chem. - Eur. J.* **2013**, *19*, 14039; p) D. A. Nagib, D. W. MacMillan, *Nature* **2011**, *480*, 224; q) D. A. Nagib, M. E. Scott, D. W. MacMillan, *J. Am. Chem. Soc.* **2009**, *131*, 10875.
- [27] H. Gao, B. Hu, W. Dong, X. Gao, L. Jiang, X. Xie, Z. Zhang, *ACS Omega* **2017**, *2*, 3168.
- [28] Y. Gao, Y. Liu, J.-P. Wan, *J. Org. Chem.* **2019**, *84*, 2243.
- [29] Z.-W. Wang, Y. Zheng, Y.-E. Qian, J.-P. Guan, W.-D. Lu, C.-P. Yuan, J.-A. Xiao, K. Chen, H.-Y. Xiang, H. Yang, *J. Org. Chem.* **2022**, *87*, 1477.
- [30] a) S. Zhang, S. Liu, Y. Sun, S. Li, J. Shi, Z. Jiang, *Chem. Soc. Rev.* **2021**, *50*, 13449; b) Z. C. Litman, Y. Wang, H. Zhao, J. F. Hartwig, *Nature* **2018**, *560*, 355.
- [31] J.-Y. Hu, Z.-B. Xie, J. Tang, Z.-G. Le, Z.-Q. Zhu, *J. Org. Chem.* **2022**, *87*, 14965.
- [32] a) Q. Jiang, J. Luo, X. Zhao, *Green Chem.* **2024**, *26*, 1846; b) H. Yu, F. Xu, *Beilstein J. Org. Chem.* **2023**, *19*, 1259; c) T. Tian, Z. Li, C.-J. Li, *Green Chem.* **2021**, *23*, 6789; d) S. A. Girard, T. Knauber, C.-J. Li, *Angew. Chem., Int. Ed.* **2014**, *53*, 74; e) C. S. Yeung, V. M. Dong, *Chem. Rev.* **2011**, *111*, 1215; f) C. J. Scheuermann, *Chem. Asian J.* **2010**, *5*, 436.
- [33] L. Fu, Z. Xu, J.-P. Wan, Y. Liu, *Org. Lett.* **2020**, *22*, 9518.
- [34] Z.-Q. Zhu, J.-Y. Hu, Z.-B. Xie, Z.-G. Le, *Chem. Commun.* **2024**, *60*, 106.
- [35] N. Talpada, A. S. Sharma, V. S. Sharma, R. Ahmed, H. Mali, P. S. Shrivastav, A. A. Sudhakar, R. S. Varma, *Chem. Nano. Mat.* **2024**, *10*, e202300641.
- [36] W. Zhao, Z. He, X. Yang, Y. Yu, J. B. Baell, F. Huang, *J. Org. Chem.* **2023**, *88*, 13634.
- [37] M. Das, M. Manik, U. Banik, P. S. Ghosh, P. Sarkar, *Intl. J. Pharma. Sci. Res.* **2014**, *5*, 3840.
- [38] Y. Bai, M. Yang, S.-X. Lin, R. A. Borse, M. B. Thoke, D. Yuan, *Tetrahedron Lett.* **2023**, *121*, 154481.
- [39] X. Fan, C. He, M. Ji, X. Sun, H. Luo, C. Li, H. Tong, W. Zhang, Z. Sun, W. Chu, *Chem. Commun.* **2022**, *58*, 6348.
- [40] C. Ma, H. Meng, X. He, Y. Jiang, B. Yu, *Front. Chem.* **2022**, *10*, 953978.
- [41] H. Dong, C. Chen, J. Zhao, Y. Ji, W. Yang, *Molecules* **2023**, *28*, 4436.
- [42] a) I. Cazin, E. Rossegger, G. Guedes de la Cruz, T. Griesser, S. Schlögl, *Polymers* **2021**, *13*, 56; b) J. Dandriyal, R. Singla, M. Kumar, V. Jaitak, *Eur. J. Med. Chem.* **2016**, *119*, 141; c) F. G. Medina, J. G. Marrero, M. Macías-Alonso, M. C. González, I. Córdova-Guerrero, A. G. T. García, S. Osegueda-Robles, *Nat. Prod. Rep.* **2015**, *32*, 1472; d) X.-M. Peng, G. L. V. Damu, C.-H. Zhou, *Curr. Pharm. Des.* **2013**, *19*, 3884; e) H. S. Jung, P. S. Kwon, J. W. Lee, J. Il Kim, C. S. Hong, J. W. Kim, S. Yan, J. Y. Lee, J. H. Lee, T. Joo, J. S. Kim, *J. Am. Chem. Soc.* **2008**, *2009*, 131. f) F. Borges, F. Roleira, N. Milhazes, L. Santana, E. Uriarte, *Curr. Med. Chem.* **2005**, *12*, 887; g) L. Santana, E. Uriarte, F. Roleira, N. Milhazes, F. Borges, *Curr. Med. Chem.* **2004**, *11*, 3239; h) M.-T. Lee, C.-K. Yen, W.-P. Yang, H.-H. Chen, C.-H. Liao, C.-H. Tsai, C. H. Chen, *Org. Lett.* **2004**, *6*, 1241.
- [43] a) A. Citarella, S. Vittorio, C. Dank, L. Ielo, *Front. Chem.* **2024**, *12*, 1362992; b) B. Borah, K. D. Dwivedi, B. Kumar, L. R. Chowhan, *Arabian J. Chem.* **2022**, *15*, 103654; c) K. Szwaczko, *Inorganics* **2022**, *10*, 23; d) V. Ortiz-de-Elguea, A. Carral-Menoyo, L. Simón-Vidal, M. Martínez-Nunes, I. Barbolla, M. G. Leite, N. Sotomayor, E. Leite, *ACS Omega* **2021**, *6*, 29483; e) M. Molnar, M. Lončarić, M. Kovač, *Curr. Org. Chem.* **2020**, *24*, 4; f) S. Chauhan, P. Verma, J. Kandasamy, V. A. Srivastava, *ChemistrySelect* **2020**, *5*, 9030.
- [44] b) R. K. Sharma, D. Katiyar, *Synthesis* **2016**, *48*, 2303.
- [45] W. Yang, S. Yang, P. Li, L. Wang, *Chem. Commun.* **2015**, *51*, 7520.
- [46] W. Fu, M. Zhu, G. Zou, C. Xu, Z. Wang, B. Ji, *J. Org. Chem.* **2015**, *80*, 4766.
- [47] M. Zhu, W. Fu, Z. Wang, C. Xua, B. Ji, *Org. Biomol. Chem.* **2017**, *15*, 9057.
- [48] S. Feng, X. Xie, W. Zhang, L. Liu, Z. Zhong, D. Xu, X. She, *Org. Lett.* **2016**, *18*, 3846.
- [49] S. Manna, K. R. Prahbu, *Org. Lett.* **2023**, *25*, 810.
- [50] P. Natarajan, Meena, P., M. Bhandari, *J. Photochem. Photobiol. A: Chem.* **2024**, *453*, 115632.
- [51] G. Qiu, T. Liu, Q. Ding, *Org. Chem. Front.* **2016**, *3*, 510.
- [52] a) E. Negishi, L. Anastasia, *Chem. Rev.* **2003**, *103*, 1979; b) N. Miyaura, A. Suzuki, *Chem. Rev.* **1995**, *95*, 2457; c) R. F. Heck, *Org. React.* **1982**, *27*, 345; d) A. Suzuki, *Acc. Chem. Res.* **1982**, *15*, 178; e) E. Negishi, *Acc. Chem. Res.* **1982**, *15*, 340; g) R. F. Heck, *Acc. Chem. Res.* **1979**, *12*, 146.
- [53] a) K. M. Kim, K. H. Chung, J. N. Kim, E. K. Ryu, *Synthesis* **1993**, 283; b) R. Benhida, P. Blanchard, J.-L. Fourrey, *Tetrahedron Lett.* **1998**, *39*, 6849; c) M. S. Whitmore, N. D. Heindel, I. Jabin, C. Guillon, *J. Heterocycl. Chem.* **2001**, *38*, 909; d) R. M. Kelkar, U. K. Joshi, M. V. Paradkar, *Synthesis* **1986**, *3*, 214; e) N. J. Cussans, T. N. Huckerby, *Tetrahedron* **1975**, *31*, 2587; f) K.-M. Kim, I.-H. Park, *Synthesis* **2004**, *16*, 2641.
- [54] S. Feng, J. Li, Z. Liu, H. Sun, H. Shi, X. Wang, X. Xie, X. She, *Org. Biomol. Chem.* **2017**, *15*, 8820.
- [55] C.-Y. Yan, Z.-W. Wu, X.-Y. He, Y.-H. Ma, X.-R. Peng, L. Wang, Q.-Q. Yang, *J. Org. Chem.* **2023**, *88*, 647.
- [56] L. Chen, L. Wu, W. Duan, T. Wang, L. Li, K. Zhang, J. Zhu, Z. Peng, F. Xiong, *J. Org. Chem.* **2018**, *83*, 8607.
- [57] W. Zhang, C. Yang, Y. Pan, X. Li, J. Cheng, *Org. Biomol. Chem.* **2018**, *16*, 5788.
- [58] X. Yang, Y. Xia, J. Tong, L. Ouyanga, Y. Lai, R. Luo, J. Liao, *Org. Biomol. Chem.* **2022**, *20*, 5239.
- [59] Q. Wang, C. Yang, C. Jiang, *Org. Biomol. Chem.* **2018**, *16*, 8196.
- [60] A. Kashyap, P. P. Singh, Y. Murti, P. Gahori, S. Mahajan, H. Kandharu, P. K. Singh, V. Srivastava, *Tetrahedron Lett.* **2024**, *142*, 155099.
- [61] M.-M. Qiao, Y.-Y. Liu, S. Yao, T.-C. Ma, Z.-L. Tang, D.-Q. Shi, W.-J. Xiao, *J. Org. Chem.* **2019**, *84*, 6798.



- [62] K. Zhang, L. Qiao, J. Xie, Z. Lin, H. Li, P. Lu, Y. Wang, *J. Org. Chem.* **2021**, *86*, 9552.
- [63] Y.-Z. Hu, Z.-P. Ye, P.-J. Xia, D. Song, X.-J. Li, Z.-L. Liu, F. Liu, K. Chen, H.-Y. Xiang, H. Yang, *J. Org. Chem.* **2021**, *86*, 4245.
- [64] J. K. Kim, Y. Liu, M. Gong, Y. Li, M. Huang, Y. Wu, *Tetrahedron Lett.* **2023**, *132*, 133249.
- [65] S. Yadav, M. Srivastava, P. Rai, J. Singh, K. P. Tiwari, J. Singh, *New J. Chem.* **2015**, *39*, 4556.
- [66] a) M. Yamaji, Y. Hakoda, H. Okamoto, F. Tanid, *Photochem. Photobiol. Sci.* **2017**, *16*, 555; b) C. Sun, Y. Bai, Y. Li, D. Liu, B. Xu, Q. Wang, *J. Mol. Model.* **2016**, *22*, 277; c) M. Tasiar, D. Kim, S. Singha, M. Krzeszewski, K. H. Ahn, D. T. Gryko, *J. Mater. Chem. C* **2015**, *3*, 1421; d) R. J. Cave, K. Burke, E. W. Castner, Jr., *J. Phys. Chem. A* **2002**, *106*, 9294.
- [67] H. Docherty, T. M. Lister, G. Mcarthur, M. T. Findlay, P. Domingo-Legarda, J. Kenyon, S. Choudhary, I. Larrosa, *Chem. Rev.* **2023**, *123*, 7692.
- [68] D. Kang, K. Ahn, S. Hong, *Asian J. Org. Chem.* **2018**, *7*, 1136.
- [69] S. M. Tomé, A. M. S. Silva, C. M. M. Santos, *Curr. Org. Synth.* **2014**, *11*, 317.
- [70] S. Mkrtchyan, V. O. Iaroshenko, *J. Org. Chem.* **2020**, *85*, 7152.
- [71] D. M. Kitcatt, S. Nicolle, A.-L. Lee, *Chem. Soc. Rev.* **2022**, *51*, 1415.
- [72] A. L. G. Kanegusuku, J. L. Roizen, *Angew. Chem., Int. Ed.* **2021**, *60*, 21116.
- [73] F. Lima, U. K. Sharma, L. Grunenber, D. Saha, S. Johannsen, J. Sedelmeier, E. V. Van der Eycken, S. V. Ley, *Angew. Chem.* **2017**, *129*, 15332.
- [74] M. E. Bungihan, M. A. Tan, M. Kitajima, N. Kogure, S. G. Franzblau, T. E. de la Cruz, H. Takayama, M. G. Nonato, *J. Nat. Med.* **2011**, *65*, 606.
- [75] K. Uchida, Y. Kawamoto, T. Kobayashi, H. Ito, *Tetrahedron Lett.* **2020**, *61*, 152611.
- [76] Z. Lu, M. Shen, T. P. Yoon, *J. Am. Chem. Soc.* **2011**, *133*, 1162.
- [77] C. Wang, X. Ren, H. Xie, Z. Lu, *Chem. - Eur. J.* **2015**, *21*, 9676.
- [78] A. G. Amador, E. M. Sherbrook, T. P. Yoon, *J. Am. Chem. Soc.* **2016**, *138*, 4722.
- [79] E. Kowalska, M. Dyguda, A. Artelska, A. Albrecht, *J. Org. Chem.* **2023**, *88*, 16589.
- [80] X. Zhou, B. Zhang, P. Wu, W. Xu, R. Wang, J. Li, H. Zhai, B. Cheng, T. Wang, *Org. Lett.* **2023**, *25*, 7512.
- [81] C. Wang, J. He, H. Mei, A. Makarem, J. Han, *J. Org. Chem.* **2024**, *89*, 5619.
- [82] P. Nanjan, J. Nambiar, B. G. Nair, A. Banerji, *Bioorg. Med. Chem.* **2015**, *23*, 3781.
- [83] M. Soto, R. G. Soengas, A. M. S. Silva, V. Gotor-Fernández, H. Rodríguez-Solla, *Chem.-Eur. J.* **2019**, *25*, 13104.
- [84] D. Fregoso-López, L. D. Miranda, *Org. Lett.* **2022**, *24*, 8615.
- [85] S. Singh, R. P. Singh, *Org. Biomol. Chem.* **2022**, *20*, 7891.
- [86] H. Zhou, X. Deng, Z. Ma, A. Zhang, Q. Qin, R. X. Tan, S. Yu, *Org. Biomol. Chem.* **2016**, *14*, 6065.
- [87] M. Mandal, G. Brahmachari, *J. Org. Chem.* **2022**, *87*, 4777.
- [88] K. N. Tripathi, M.d. Belal, R. P. Singh, *J. Org. Chem.* **2020**, *85*, 1193.
- [89] M. Moczulski, E. Kowalska, E. Kusmierek, Ł. Albrecht, A. Albrecht, *RSC Adv.* **2021**, *11*, 27782.
- [90] E. Kowalska, A. Artelska, A. Albrecht, *J. Org. Chem.* **2022**, *87*, 9645.
- [91] E. Babaei, T. T. Küçükılınç, L. Jalili-Baleh, H. Nadri, E. Öz, H. Forootanfar, E. Hosseinzadeh, T. Akbari, M. S. Ardestani, L. Firoozpour, A. Foroumadi, M. Sharifzadeh, B. B. F. Mirjalili, M. Khoobi, *Front. Chem.* **2022**, *10*, 895483.
- [92] K. Armendariz-Barrientos, L. A. Pérez, S. Lagunas-Rivera, Y. Alcaraz-Contreras, M. A. García-Revilla, H. Prado-García, R. García-Becerra, M. A. Vázquez, *Results Chem.* **2025**, *13*, 101959.
- [93] T. Morofuji, Y. Matsui, M. Ohno, G. Ikarashi, N. Kano, *Chem.-Eur. J.* **2021**, *27*, 6713.
- [94] D. M. Kitcatt, K. A. Scott, E. Rongione, S. Nicolleb, A.-L. Lee, *Chem. Sci.* **2023**, *14*, 9806.
- [95] S. Singh, R. P. Singh, *Synthesis* **2025**, *57*, 481.
- [96] E. Quezada, C. Picciau, G. Delogu, F. Orallo, L. Santana, E. Uriarte, *Bioorg. Med. Chem. Lett.* **2009**, *19*, 326.
- [97] S. M. Ghouse, K. Bahatam, A. Angeli, G. Pawar, K. K. Chinchilli, V. M. Yaddanapudi, A. Mohammed, C. T. Supuran, S. Nanduri, *J. Enzyme Inhib. Med. Chem.* **2023**, *38*, 2185760.
- [98] C. Jin, Z. Yan, B. Sun, J. Yang, *Org. Lett.* **2019**, *21*, 2064.
- [99] K. Rybicka-Jasińska, B. König, D. Gryko, *Eur. J. Org. Chem.* **2017**, *2017*, 2104.
- [100] A. Moazzam, F. Jafarpour, *New J. Chem.* **2020**, *44*, 16692.

Manuscript received: January 23, 2025

Revised manuscript received: March 18, 2025

Version of record online: April 3, 2025